Detection of the Missing Baryons

Yin-Zhe Ma (马寅哲)

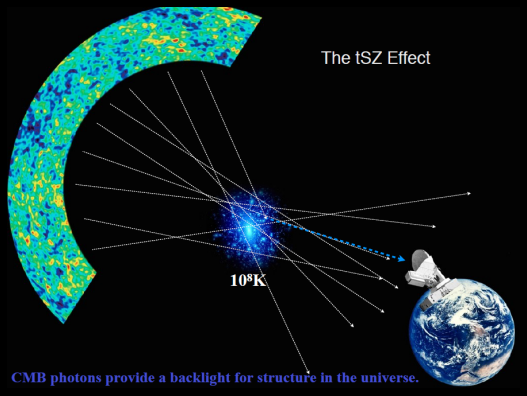

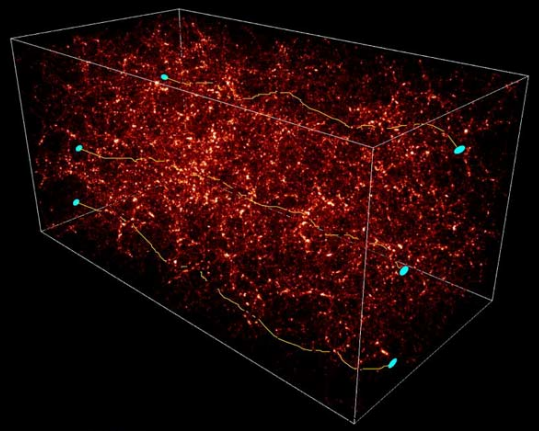

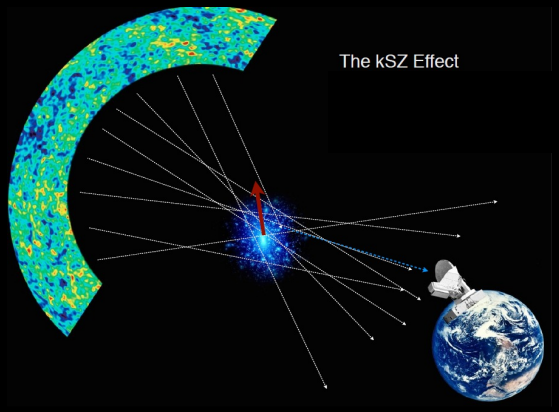

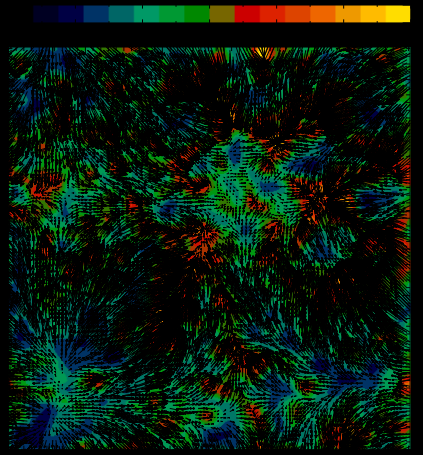

C. Hernández-Monteagudo, YZM+ Planck kSZ team

YZM, L. Van Waerbeke, G. Hinshaw, A. Hojatti, D. Scott, 2014

A. Hojatti, I. G. McCarthy, J. Harnois-Deraps, YZM, L. Van Waerbeke, G.Hinshaw, A. M. C. Le Brun , 2014

H. Tanimura, YZM, G. Hinshaw, 2015

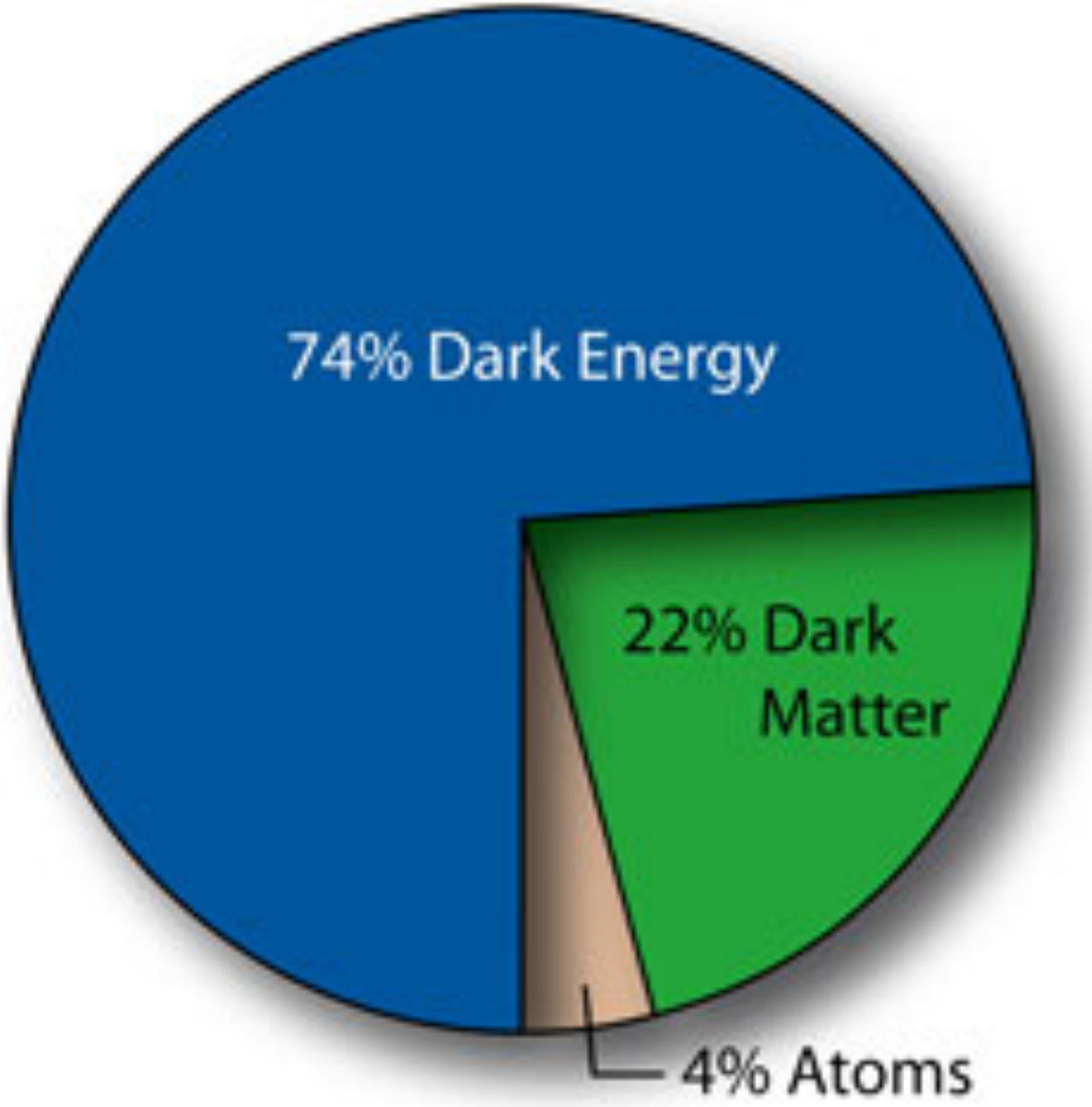
74% Dark Energy
22% Dark Matter
4% Atoms

Cosmic baryon inventory:

Category	Parameter	Components[a]
3.3.....	Main-sequence stars: spheroids and bulges	0.0015 ± 0.0004
3.4.....	Main-sequence stars: disks and irregulars	0.00055 ± 0.00014
3.5.....	White dwarfs	0.00036 ± 0.00008
3.6.....	Neutron stars	0.00005 ± 0.00002
3.7.....	Black holes	0.00007 ± 0.00002
3.8.....	Substellar objects	0.00014 ± 0.00007
3.9.....	H I + He I	0.00062 ± 0.00010
3.10.....	Molecular gas	0.00016 ± 0.00006
3.11.....	Planets	10^{-6}
3.12.....	Condensed matter	$10^{-5.6 \pm 0.3}$
3.13.....	Sequestered in massive black holes	$10^{-5.4}(1 + \epsilon_n)$

3.3+…+3.13: $\Omega_{b,g} = 0.0035$ =8% total baryon density

90% of baryons are in either intergalactic or intercluster medium

Fukugita, & Peebles 2004

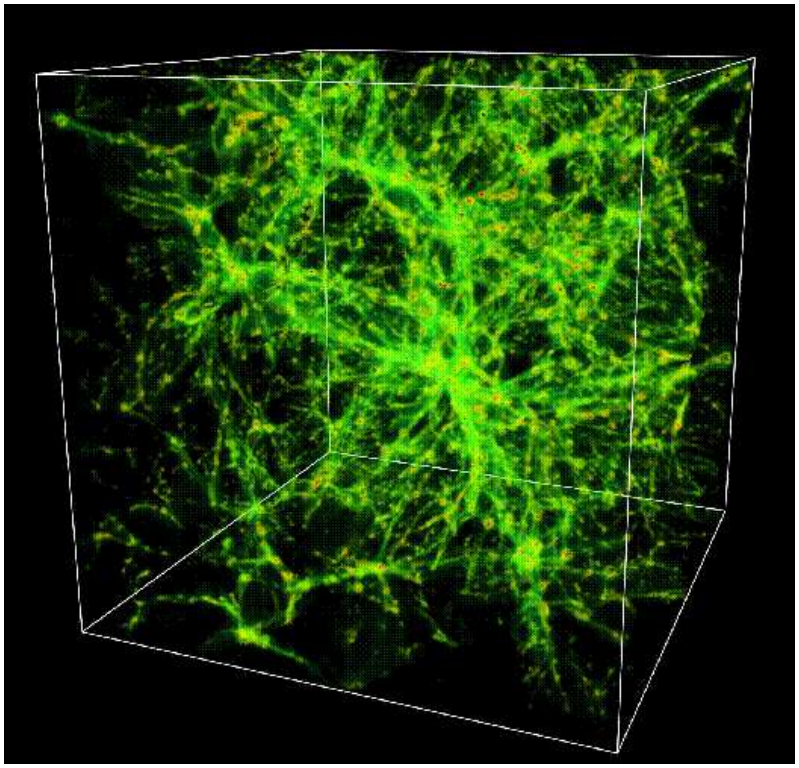

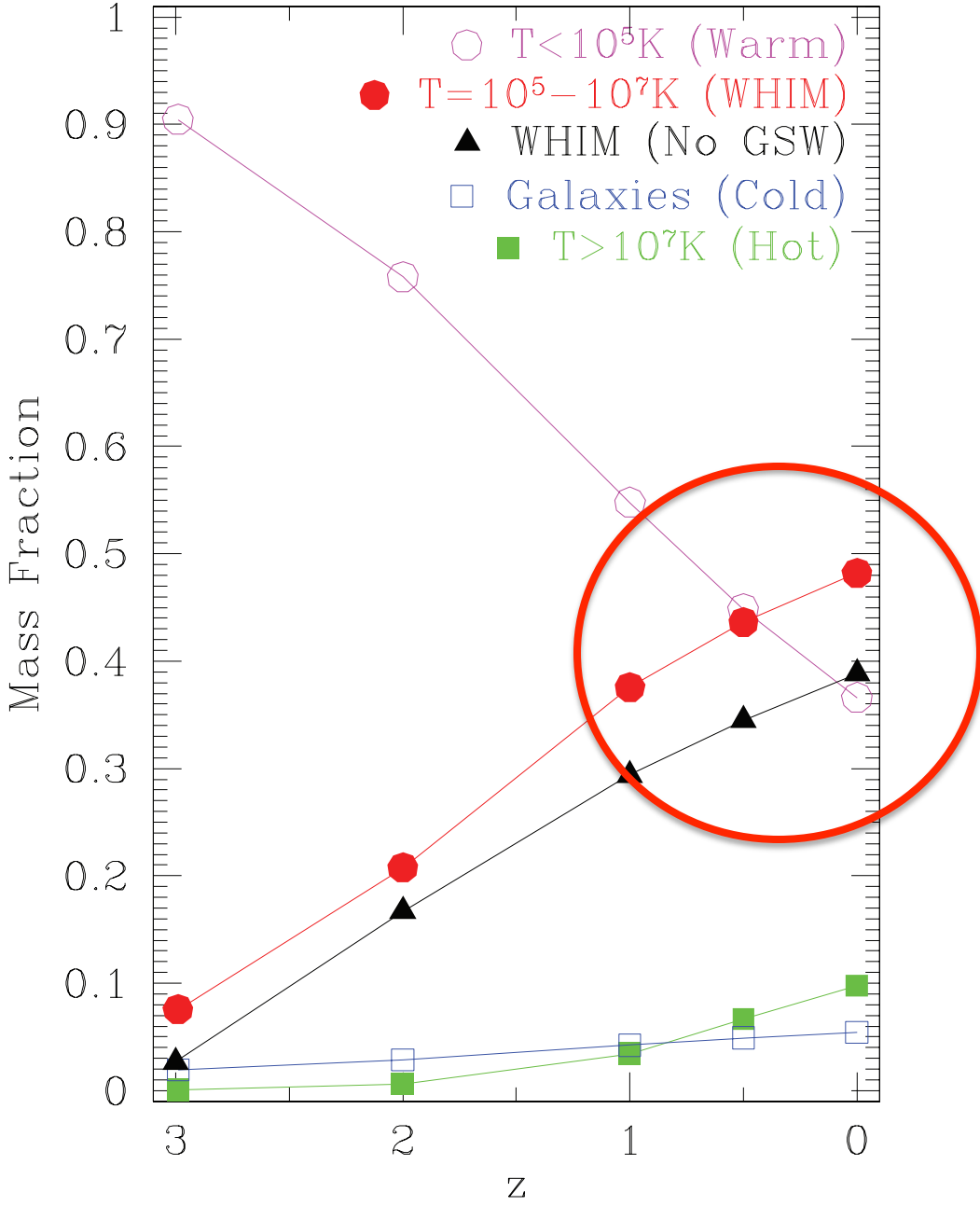

Cen and Ostriker 2006

X-ray: ~ n_e(r)^2

thermal Sunyaev-Zeldovich effect X Weak Lensing

and compare with halo model prediction and hydrodynamic simulation

kinetic Sunyaev-Zeldovich effect X Peculiar velocity field

Stacking luminous red galaxies with thermal SZ maps

The thermal Sunyaev-Zeldovich effect

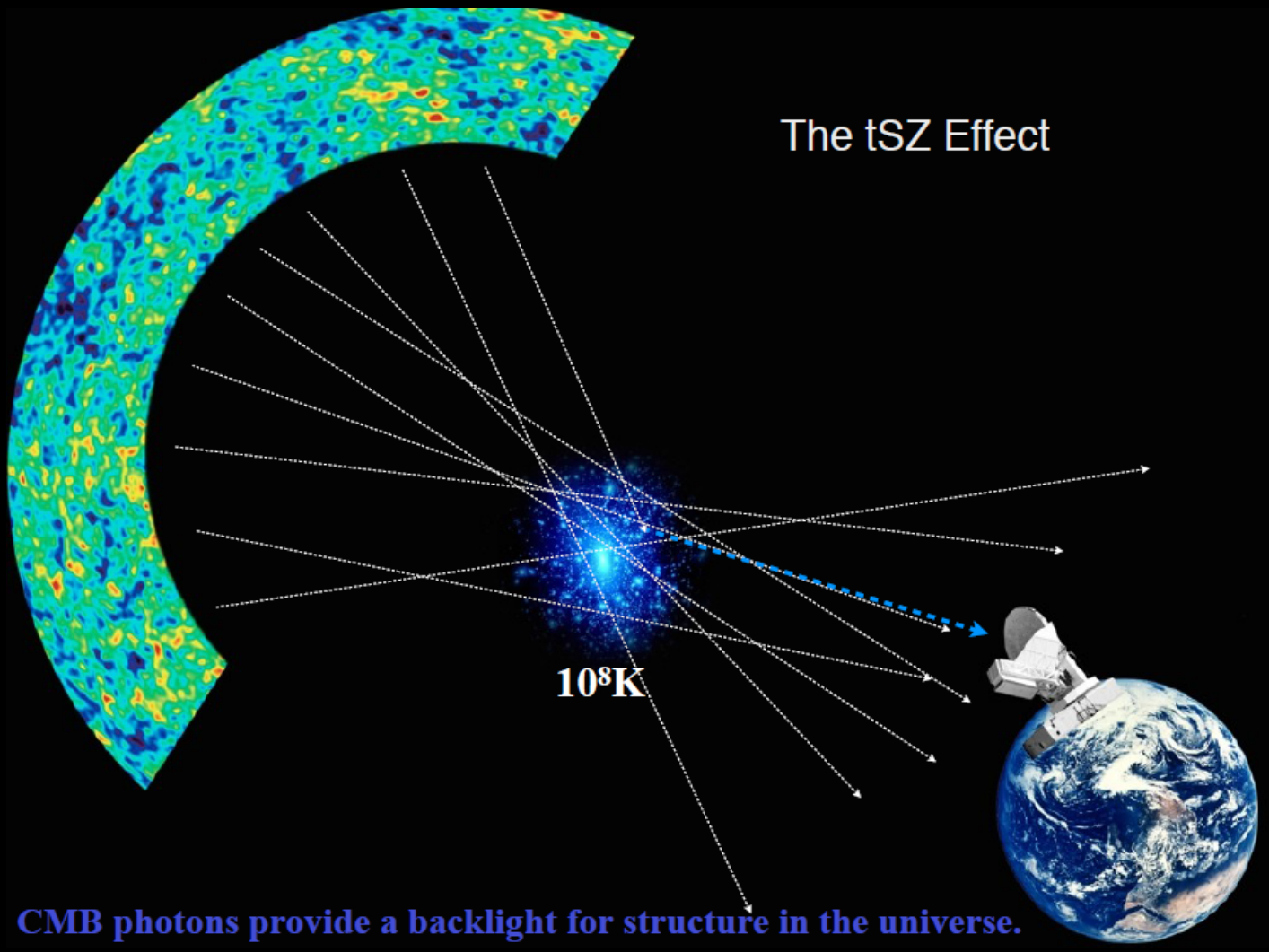

Thermal Sunyaev-Zeldovich effect (tSZ):

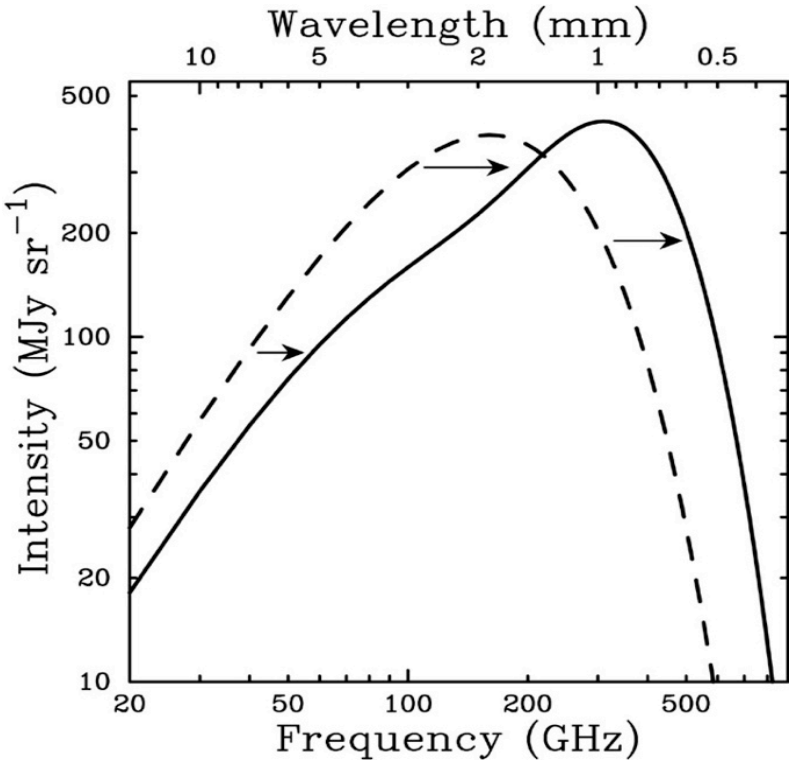

$$\frac{\Delta T}{T} = \left[\eta \frac{e^{\eta}+1}{e^{\eta}-1} - 4\right] y \equiv g_{\nu} y$$

$$g_{\nu} \equiv (\eta(e^{\eta}+1)/(e^{\eta}-1)) - 4$$

$$\eta = \frac{h\nu}{k_B T_{\mathrm{CMB}}} = \frac{h\nu_0}{k_B T_0} = 1.76 \left(\frac{\nu_0}{100\mathrm{GHz}}\right)$$

$$y = \frac{k_B \sigma_T}{m_e c^2} \int_0^l T_e(l) n_e(l)\, \mathrm{d}l$$

WMAP:

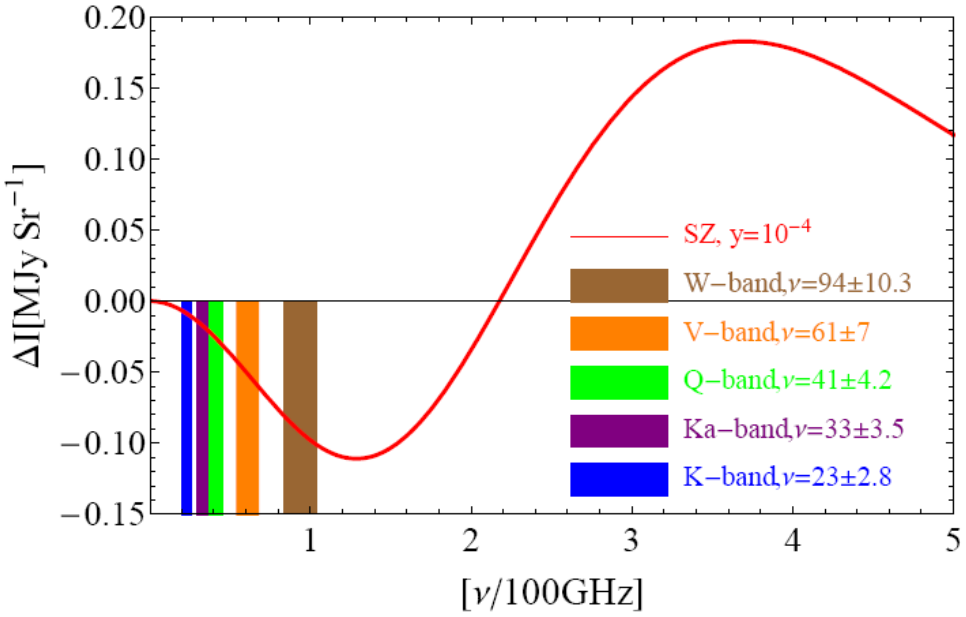
0.20
0.15
0.10
0.05
0.00
−0.05
−0.10
−0.15
ΔI[MJy Sr^{-1}]
1
2
3
4
5
[ν/100GHz]
SZ, y=10^{-4}
W−band,ν=94±10.3
V−band,ν=61±7
Q−band,ν=41±4.2
Ka−band,ν=33±3.5
K−band,ν=23±2.8

Planck:

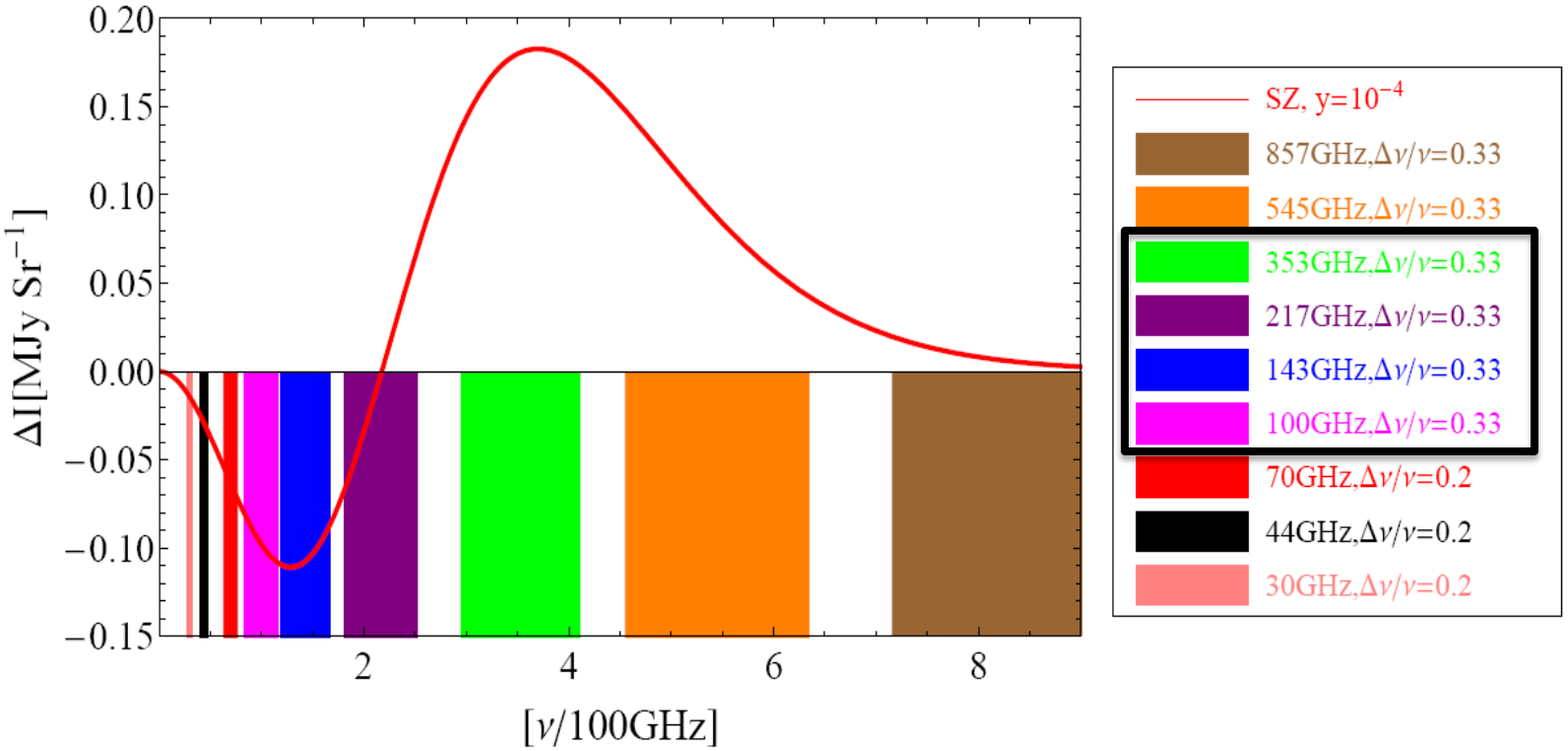
0.20
0.15
0.10
0.05
0.00
−0.05
−0.10
−0.15
ΔI[MJy Sr^{-1}]
2
4
6
8
[ν/100GHz]
SZ, y=10^{-4}
857GHz,Δν/ν=0.33
545GHz,Δν/ν=0.33
353GHz,Δν/ν=0.33
217GHz,Δν/ν=0.33
143GHz,Δν/ν=0.33
100GHz,Δν/ν=0.33
70GHz,Δν/ν=0.2
44GHz,Δν/ν=0.2
30GHz,Δν/ν=0.2

SZ map from linear combination of Planck frequency bands: ν_i = 100, 143, 217, 353 GHz.

$$T_{SZ}/T_0 \equiv y\, S_{SZ}(\nu_i) = \sum b_i\, T(\nu_i)$$

1. $\sum b_i\, S_{SZ}(\nu_i) = 1$ $\qquad$ $S_{SZ}(x) = x\, coth(x/2) - 4 \;\; (x = h\nu/kT)$

2. $\sum b_i\, S_{CMB}(\nu_i) = 0$ $\qquad$ $S_{CMB}(x) = 1$

3. $\sum b_i\, S_{''dust''}(\nu_i) = 0$ $\qquad$ $S_{''dust''}(\nu_i) = \nu^{\beta}\, g(x)$

Planck Full-Sky Maps – 9 Frequencies

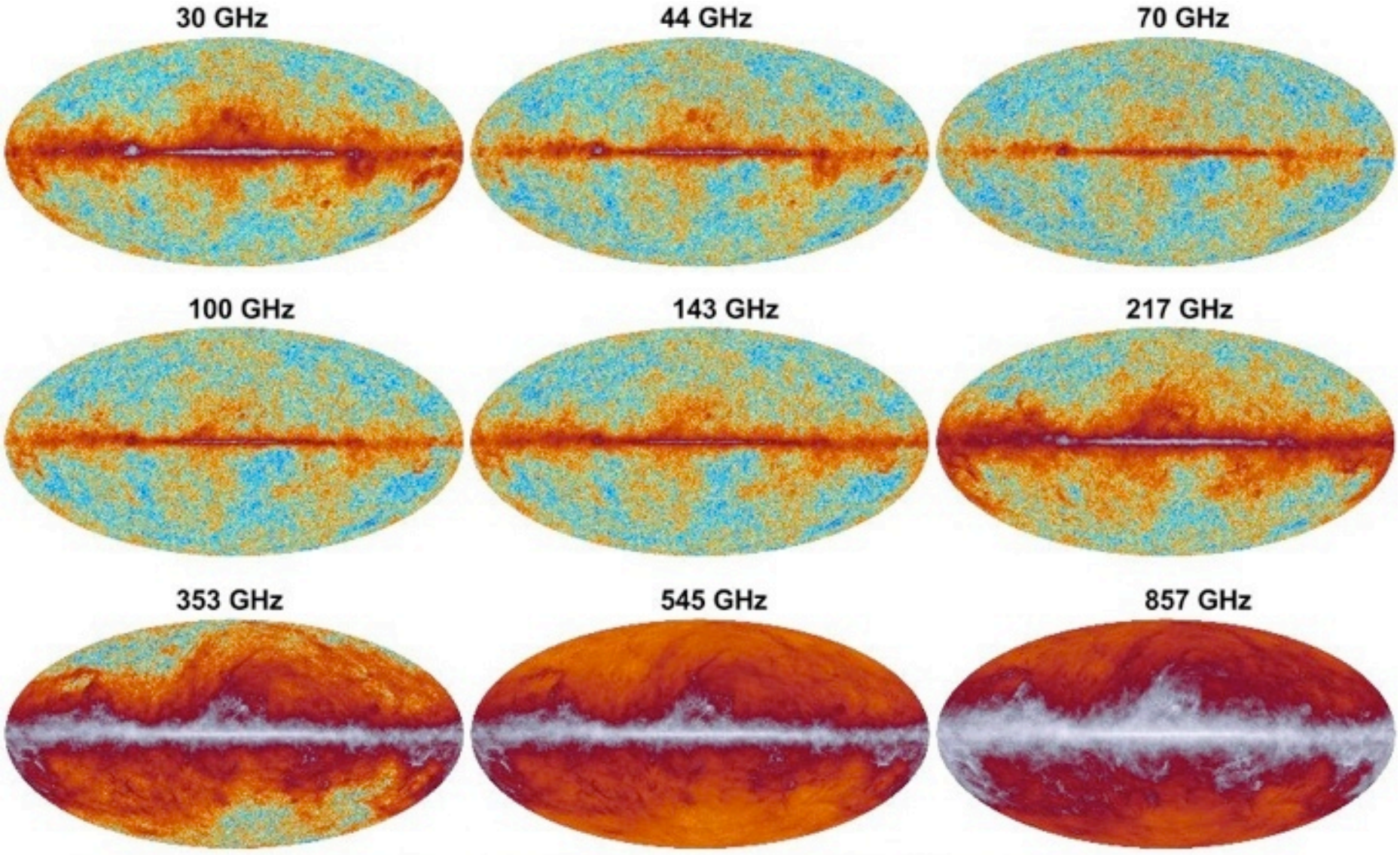

Planck Full-Sky Maps – 4 Frequencies

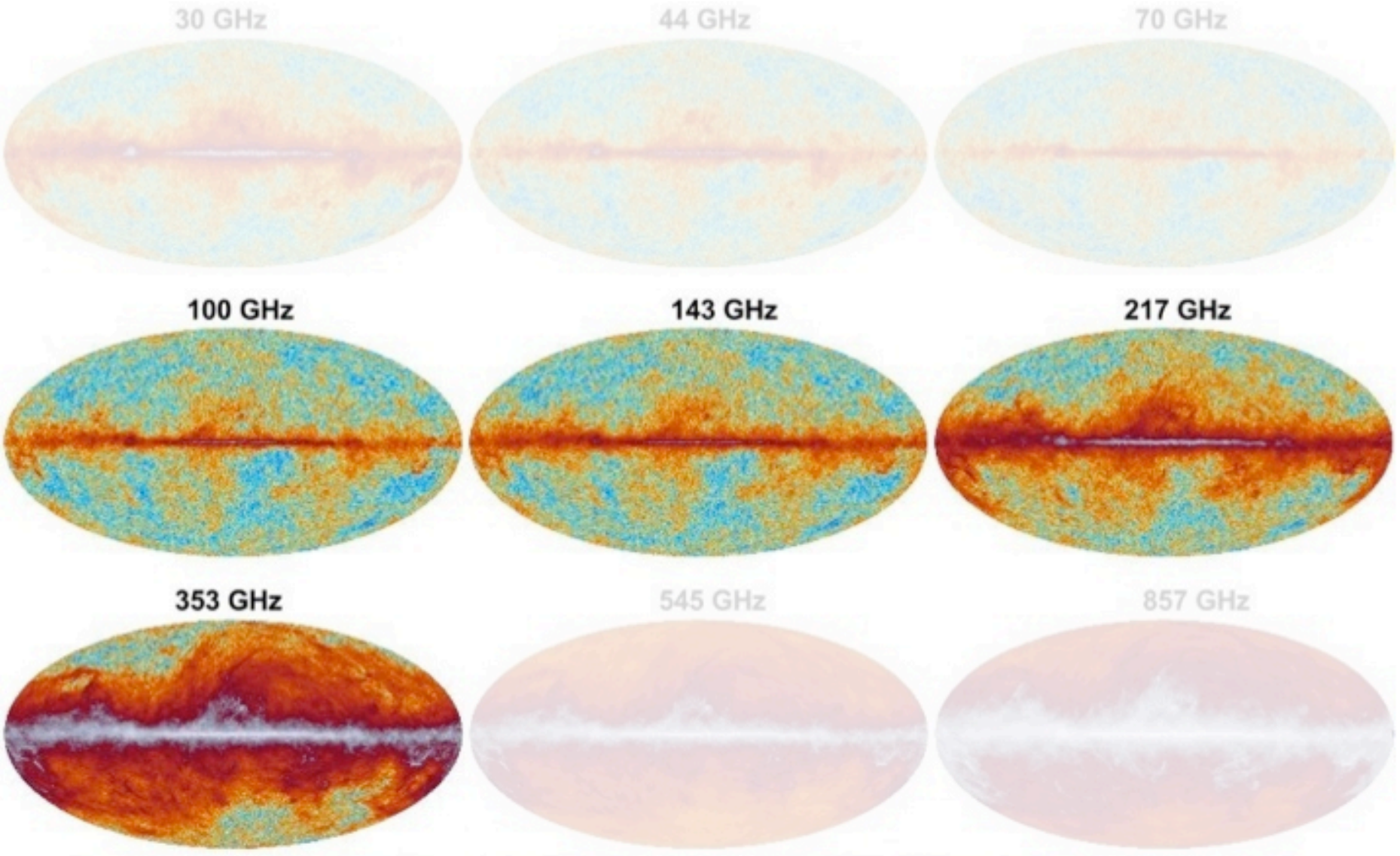

Planck SZ y map, version E

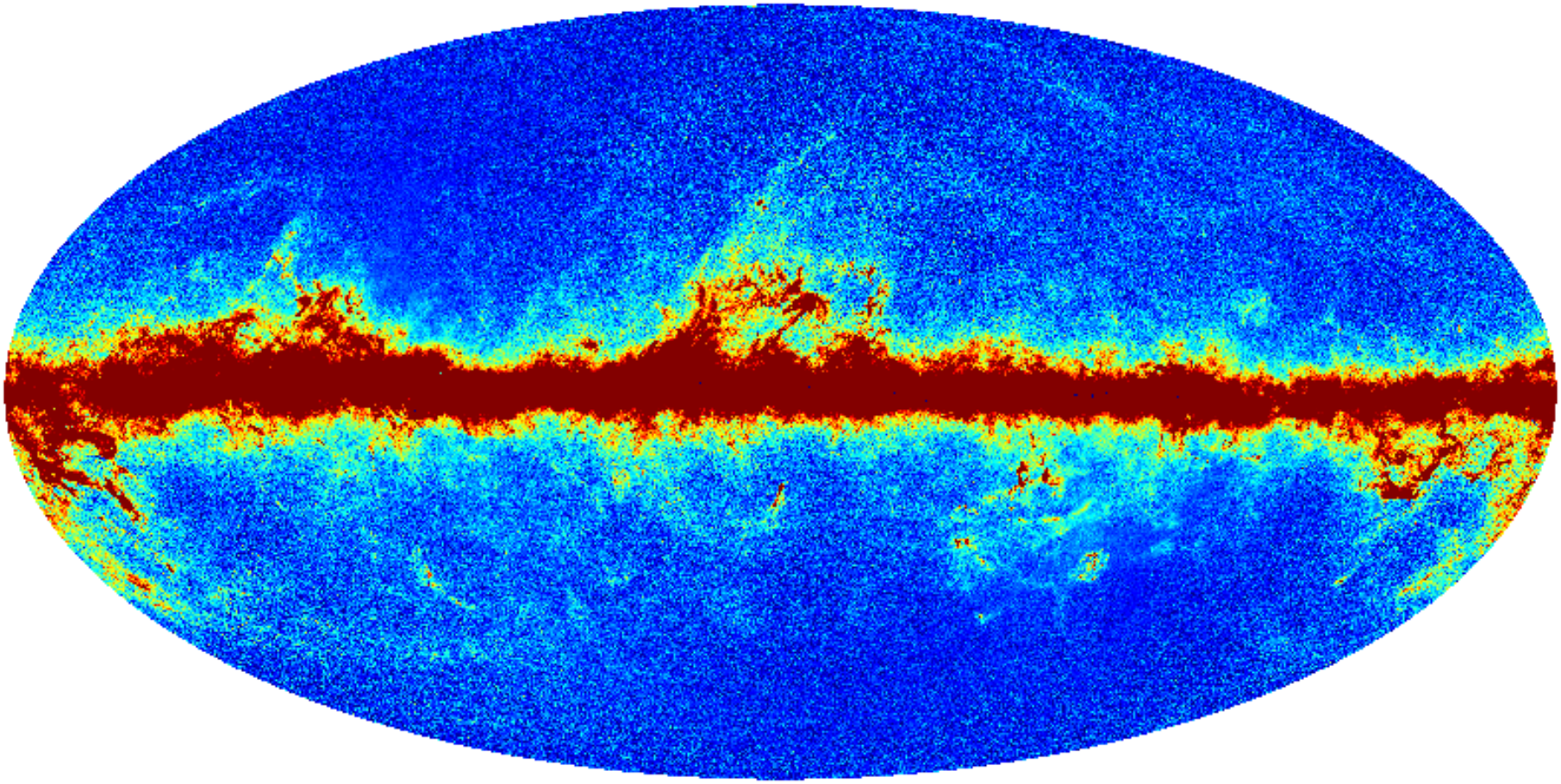

Reject $\beta_{\rm dust} = 2.0$, $r_{2.0}(100\ {\rm GHz}) = 0$

Planck SZ no-y map, version E

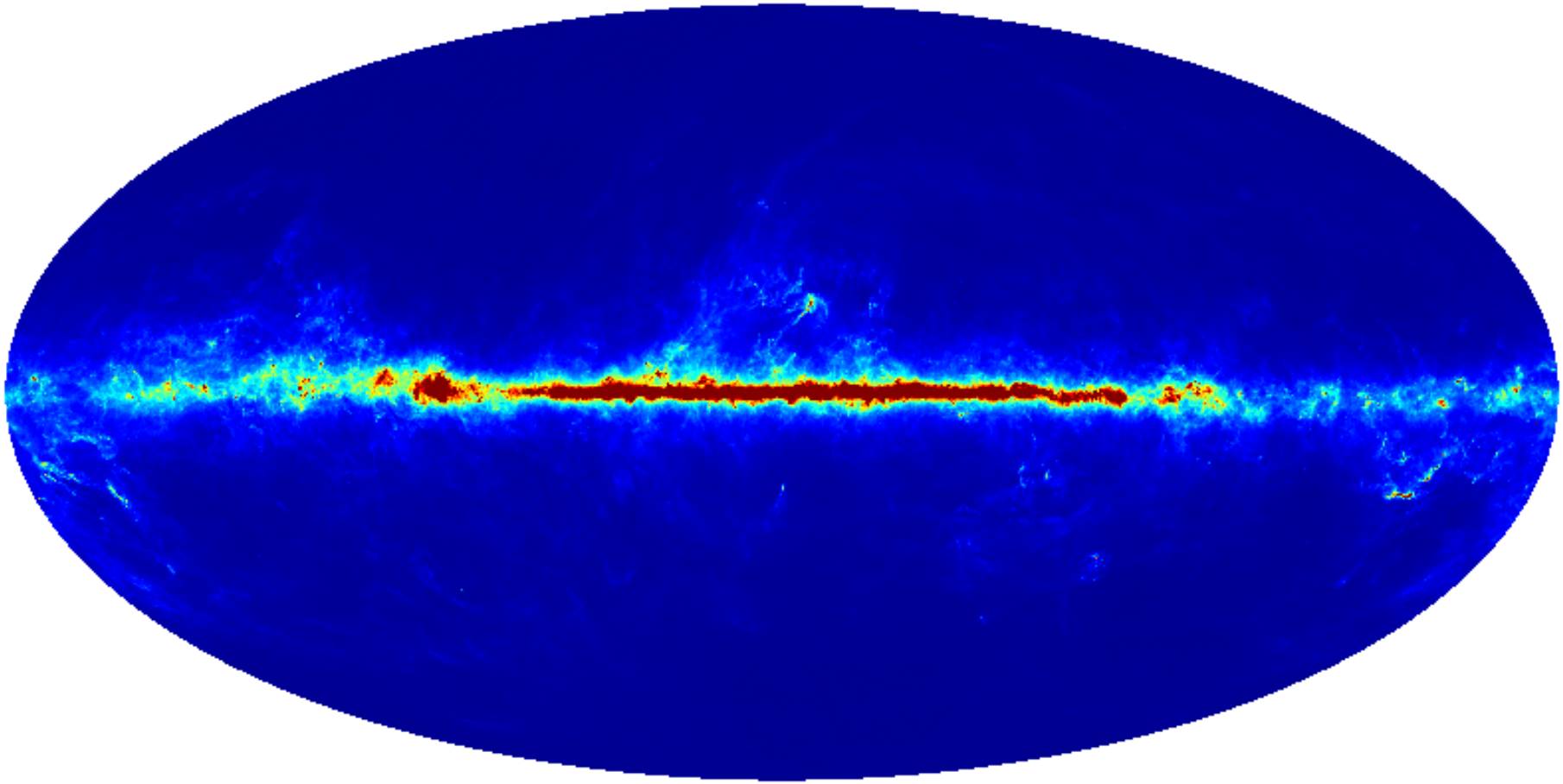

y=0 10^{-4}

Reject $S_{SZ}(\nu)$, retain $\beta_{dust} = 1.8$

CFHT mass map:

154 deg^2 in 4 patches

Van Waerbeke et al., 2014, MNRAS

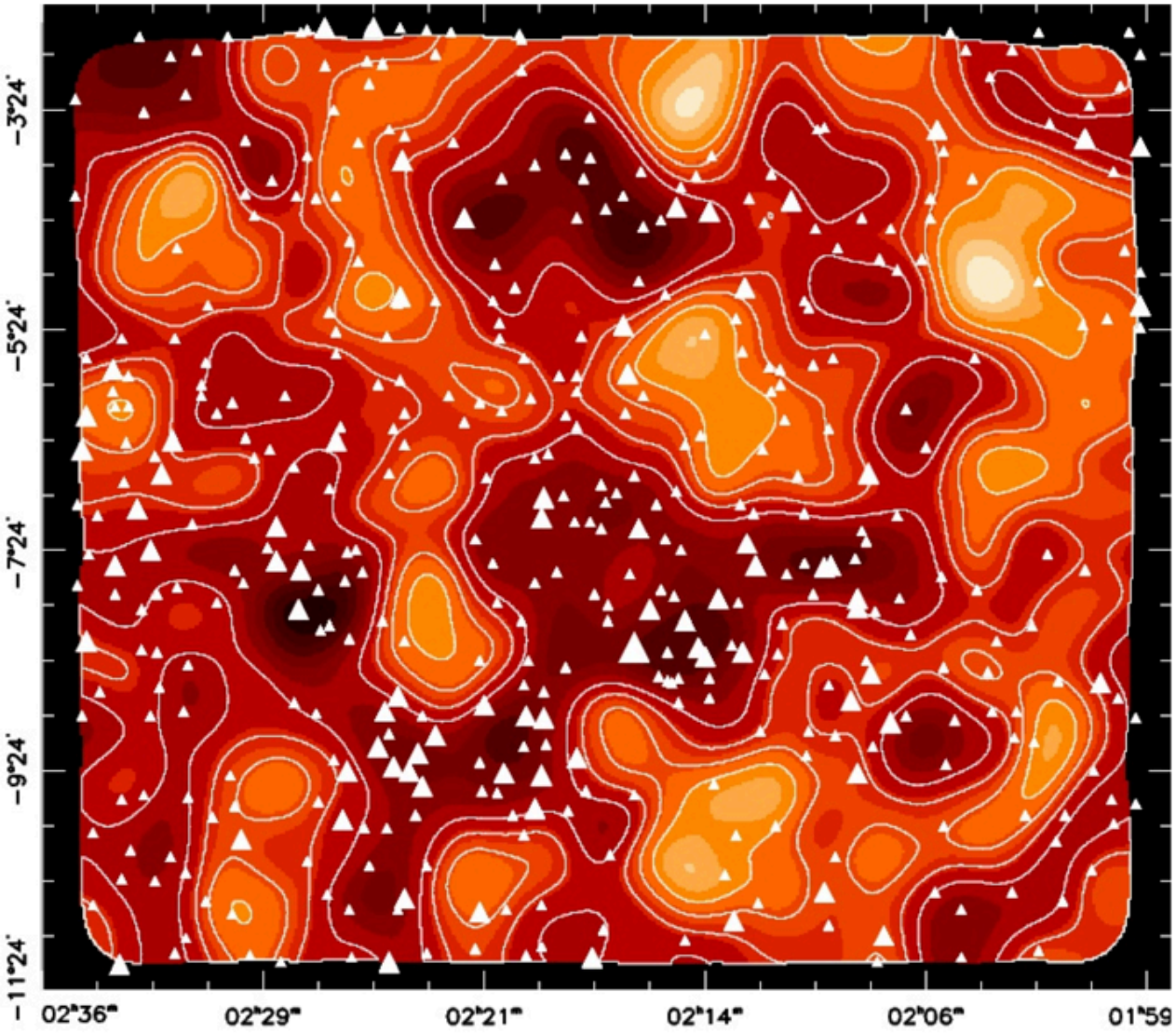

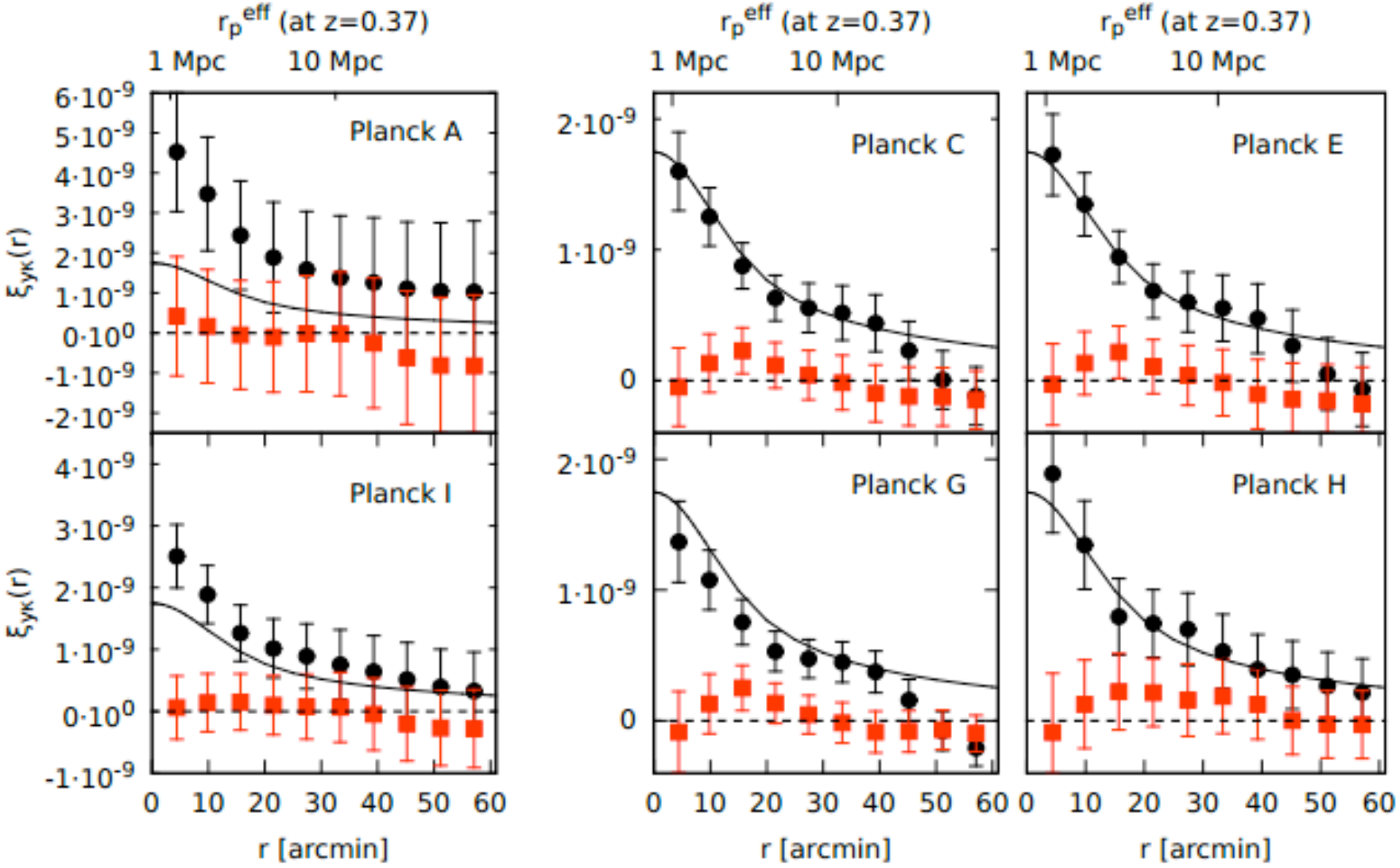

van Waerbake, Hinshaw, Murray: 2014 Phys. Rev. D

Halo model:

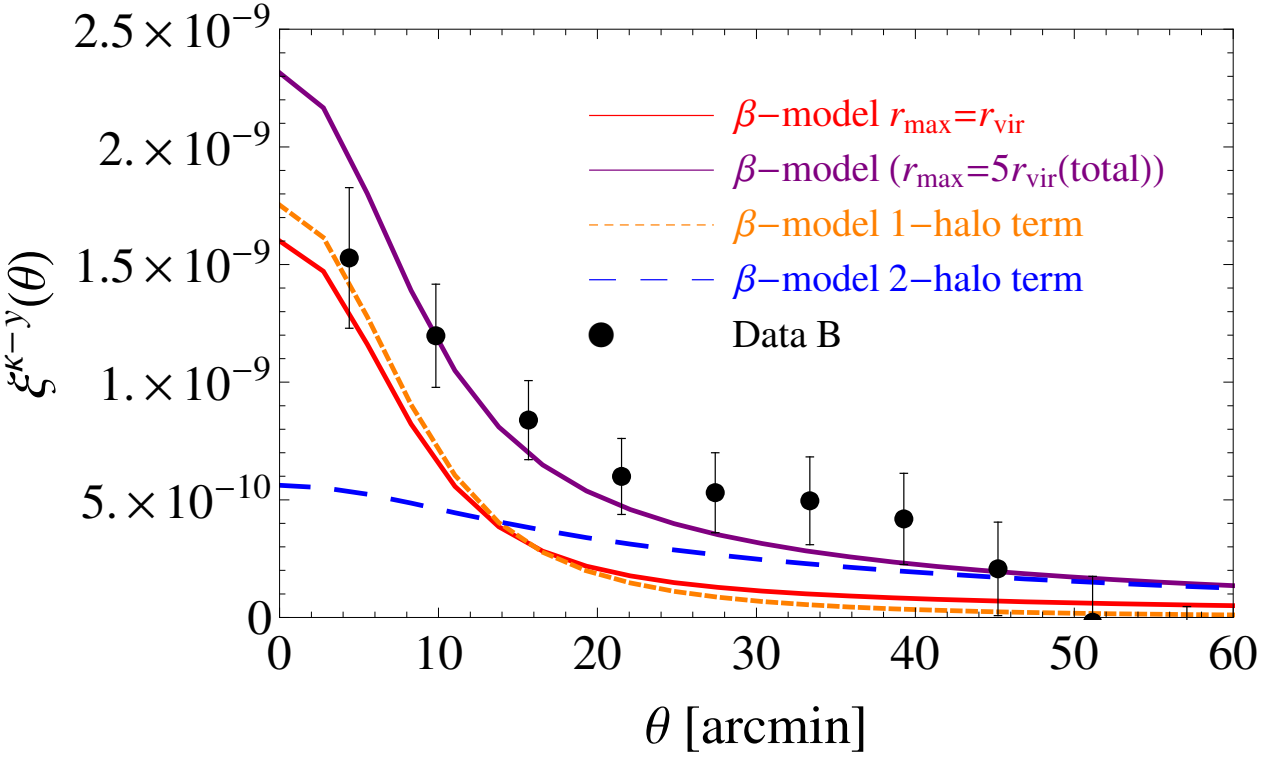

Ma et al. fits a halo model to the observed correlation function. A β model fits well, but in this context the data requires a 2-halo term to fit the large angular scale separation.

$$\chi^2(\alpha,\beta) = \sum_{ij} \left[\xi^{\rm d}(\theta_i) - \alpha\xi^{\rm 1h}(\theta_i) - \beta\xi^{\rm 2h}(\theta_i)\right] \times C_{ij}^{-1} \left[\xi^{\rm d}(\theta_j) - \alpha\xi^{\rm 1h}(\theta_j) - \beta\xi^{\rm 2h}(\theta_j)\right]$$

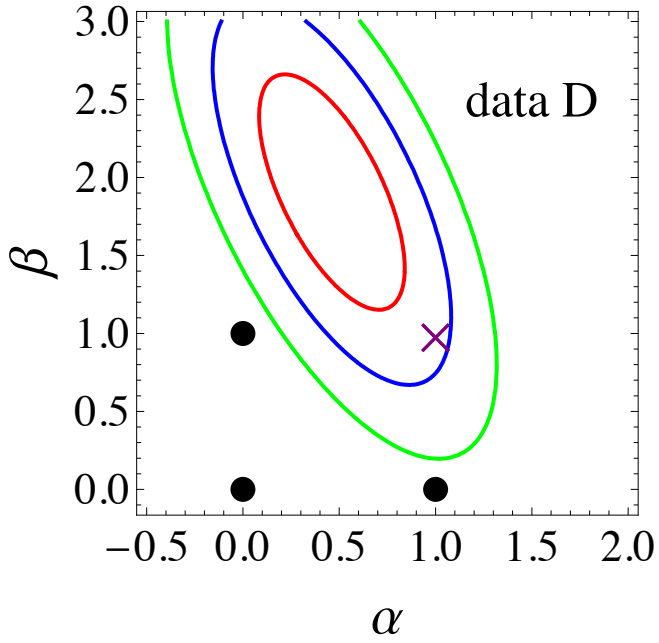

Data set	2-halo only	1-halo only	No correlation
B	7.6×10^{-5}	2.4×10^{-4}	3.8×10^{-11}
C	2.2×10^{-5}	1.0×10^{-4}	1.1×10^{-11}
D	7.1×10^{-5}	6.0×10^{-4}	6.6×10^{-11}
E	2.6×10^{-5}	2.8×10^{-4}	1.3×10^{-11}
F	1.7×10^{-3}	5.4×10^{-3}	1.5×10^{-8}
G	4.6×10^{-3}	1.0×10^{-2}	9.6×10^{-8}
H	6.7×10^{-4}	7.3×10^{-5}	1.1×10^{-9}

TABLE I: For each y-map B–H, the probability that the fit in Eq. (6) allows: $\alpha = 0, \beta = 1$ (no 1-halo term, column 2); $\alpha = 1, \beta = 0$ (no 2-halo term, column 3); and $\alpha = \beta = 0$ (no cross-correlation, column 4). We assume $P = \exp(-\Delta\chi^2/2)$.

	$10^{12}\,\mathrm{M}_\odot$–$10^{14}\,\mathrm{M}_\odot$	$10^{14}\,\mathrm{M}_\odot$–$10^{16}\,\mathrm{M}_\odot$
$(0.01\text{–}1)\,r_{\mathrm{vir}}$	26%	28%
$(1\text{–}100)\,r_{\mathrm{vir}}$	14%	32%

By applying the virial theorem with z = 0.37, for the mass range 10^12—10^16 M_sun, we get T_e = 10^5—10^8 K.

Simulation vs data

Simulation	UV/X-ray background	Cooling	Star formation	SN feedback	AGN feedback	$\Delta T_{\rm heat}$
NOCOOL	Yes	No	No	No	No	...
REF	Yes	Yes	Yes	Yes	No	...
AGN 8.0	Yes	Yes	Yes	Yes	Yes	$10^{8.0}$ K
AGN 8.5	Yes	Yes	Yes	Yes	Yes	$10^{8.5}$ K
AGN 8.7	Yes	Yes	Yes	Yes	Yes	$10^{8.7}$ K

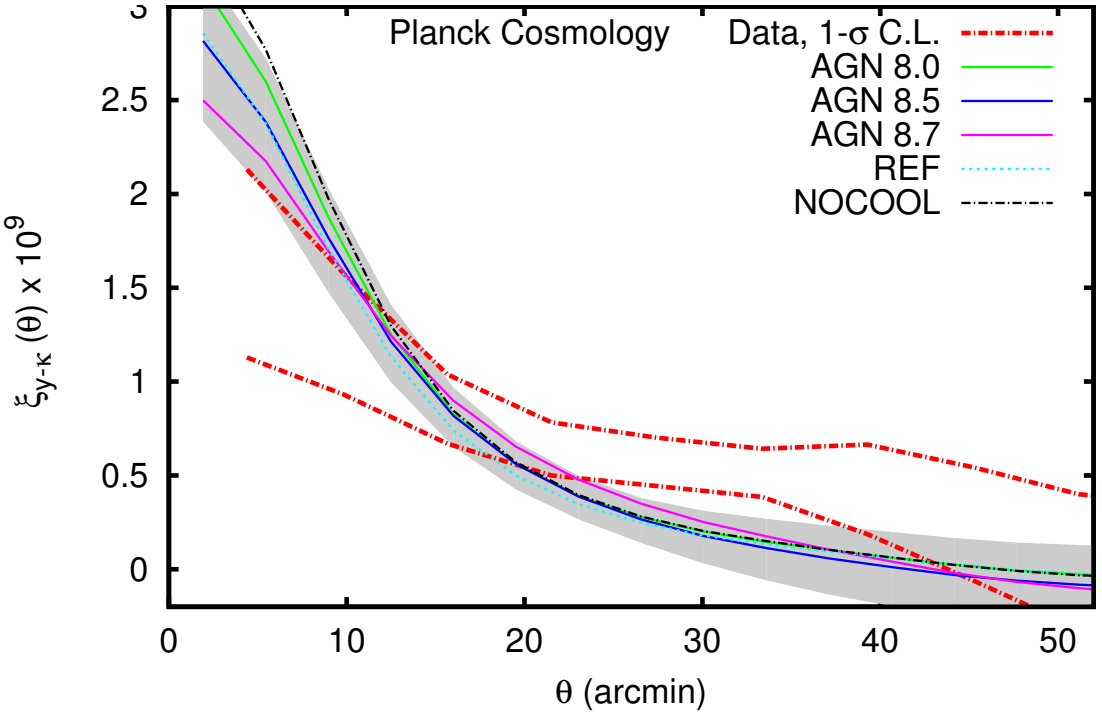

NOCOOL is a standard non-radiative ('adiabatic') model.
REF is the OWLS reference model and includes sub-grid prescriptions for star formation, metal-dependent radiative cooling, stellar evolution, mass loss, chemical enrichment, and a kinetic supernova feedback prescription.
The AGN models are built on the REF model and additionally include a prescription for black hole growth and feedback from active galactic nuclei. The three AGN models differ only in their choice of the key parameter of the AGN feedback model ΔT, which is the temperature by which neighboring gas is raised due to feedback.

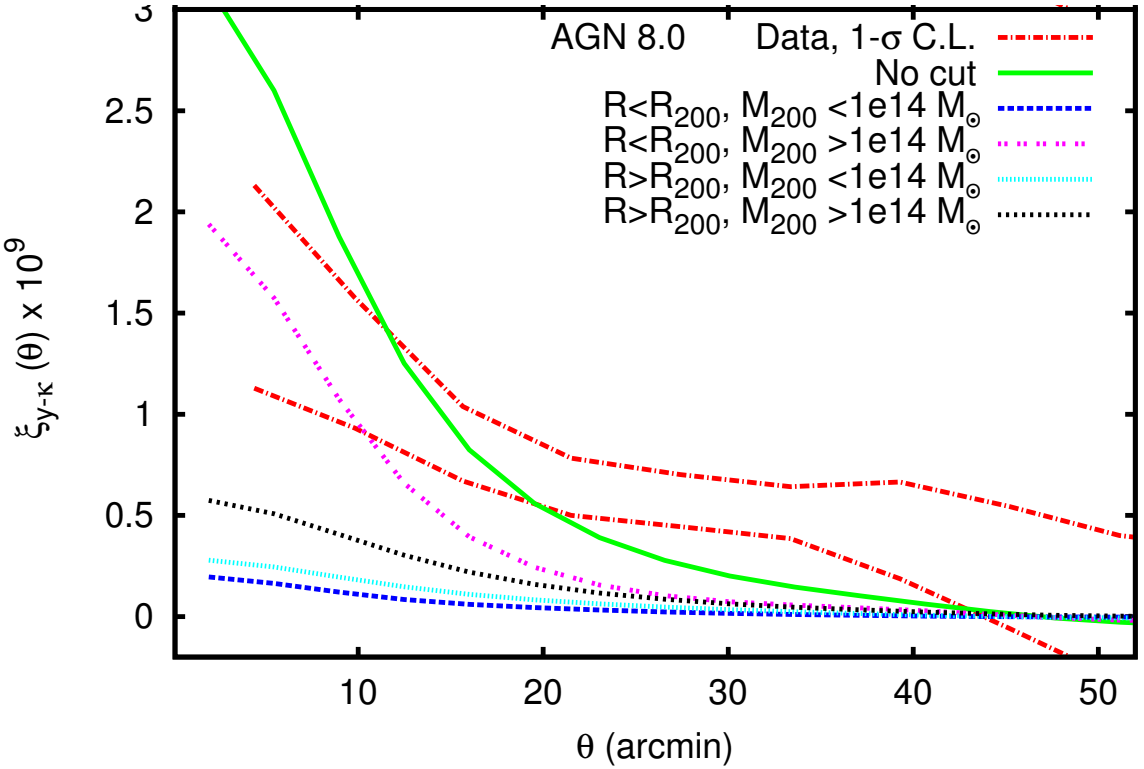

	Simulation		Halo model
Bin	Signal	Baryon	Signal
Low mass, inner radii	7%	6%	26%
Low mass, outer radii	12%	24%	14%
High mass, inner radii	56%	4%	28%
High mass, outer radii	25%	7%	32%

Evidence of gas outside the virial radius

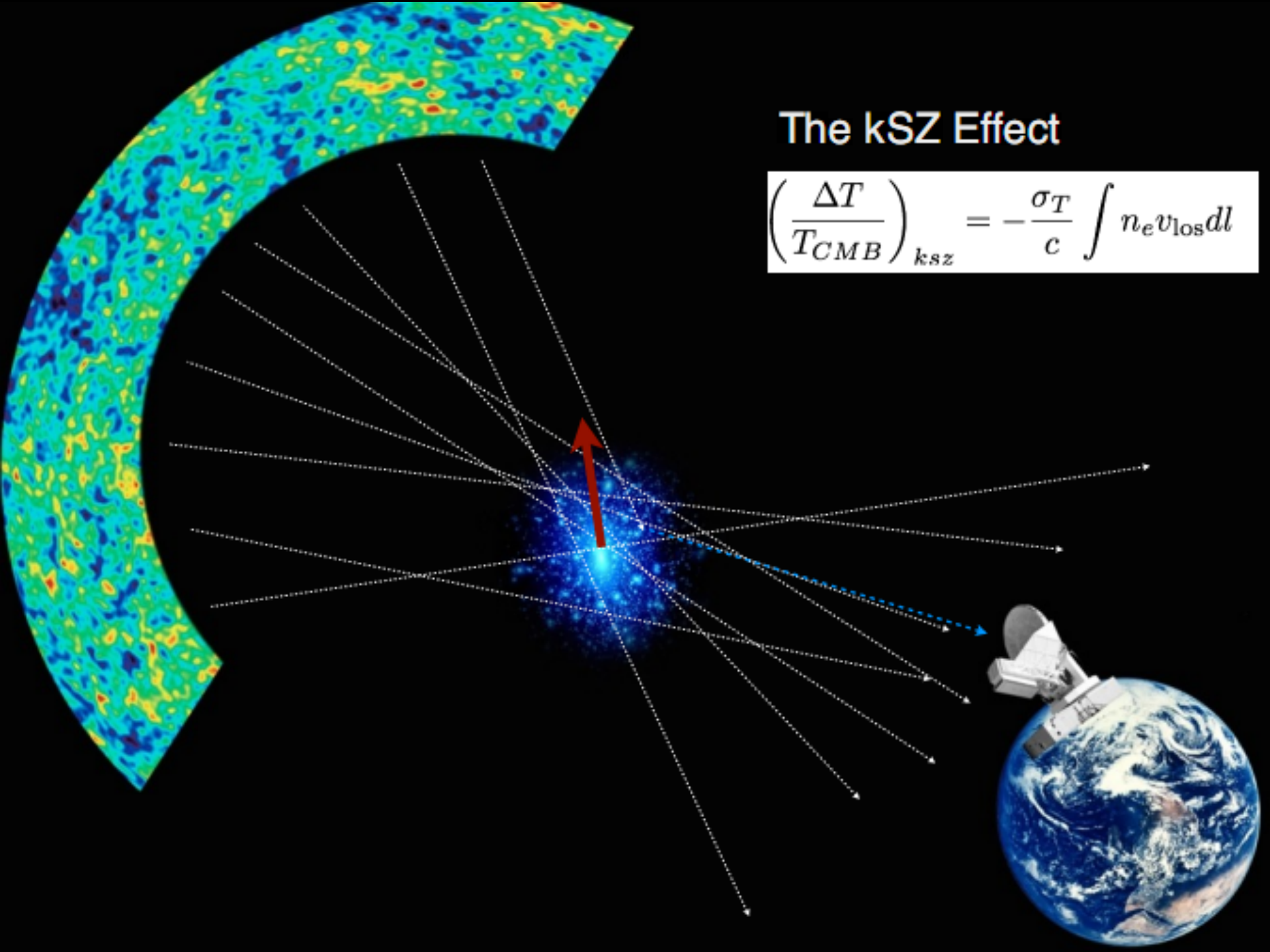
The kSZ Effect
$\left(\frac{\Delta T}{T_{CMB}}\right)_{ksz} = -\frac{\sigma_T}{c}\int n_e v_{\rm los} dl$

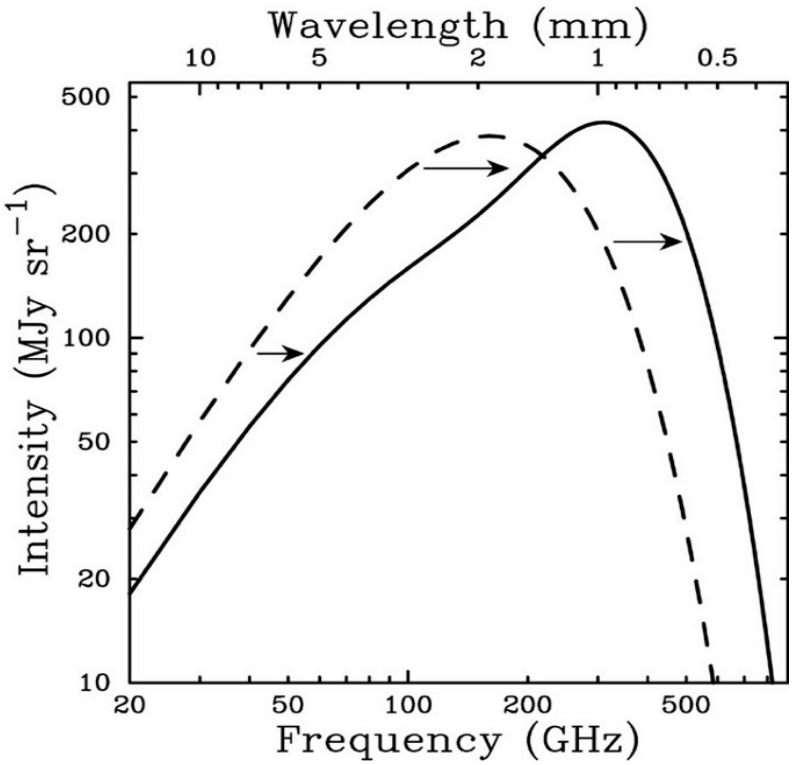

$$\frac{\Delta T}{T} = \left[\eta \frac{e^{\eta}+1}{e^{\eta}-1} - 4\right] y \equiv g_{\nu} y$$

tSZ:

$$g_{\nu} \equiv (\eta(e^{\eta}+1)/(e^{\eta}-1)) - 4$$

$$\eta = \frac{h\nu}{k_B T_{\mathrm{CMB}}} = \frac{h\nu_0}{k_B T_0} = 1.76 \left(\frac{\nu_0}{100\mathrm{GHz}}\right)$$

$$y = \frac{k_B \sigma_T}{m_e c^2} \int_0^l T_e(l) n_e(l)\, \mathrm{d}l$$

kSZ:

$$\frac{\delta T}{T_0}(\hat{\boldsymbol{n}}) = -\int \mathrm{d}l\, \sigma_{\mathrm{T}} n_{\mathrm{e}} \left(\frac{\boldsymbol{v}}{c} \cdot \hat{\boldsymbol{n}}\right)$$

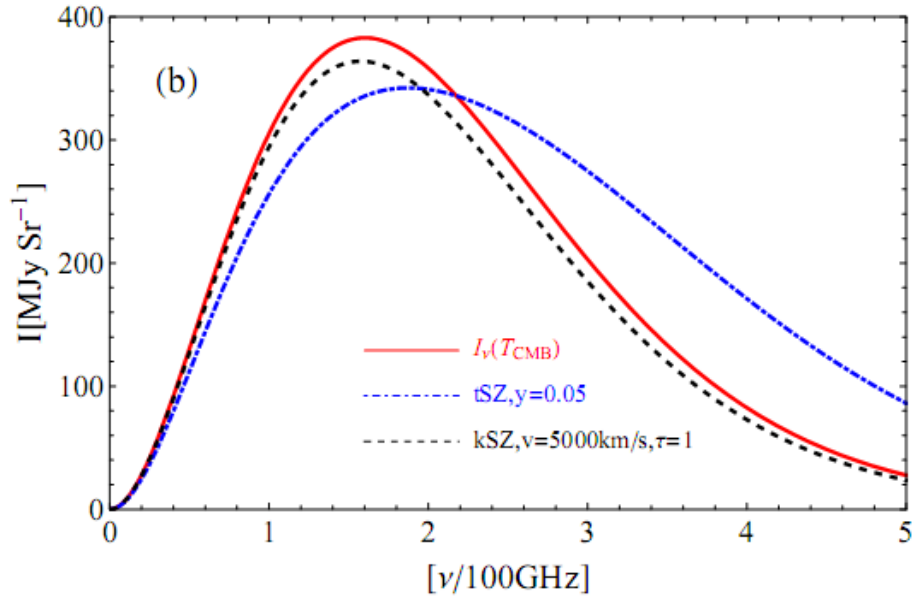

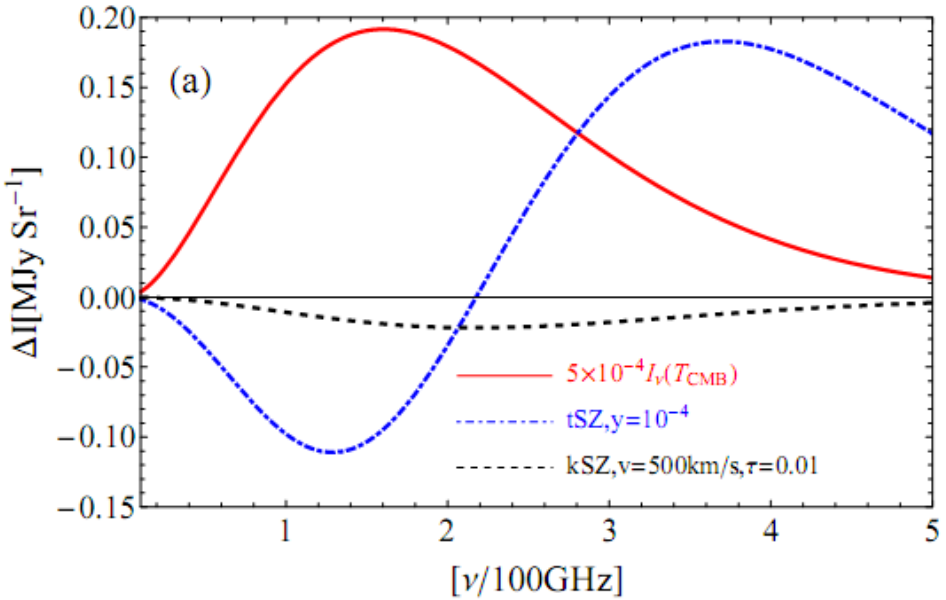

WMAP:

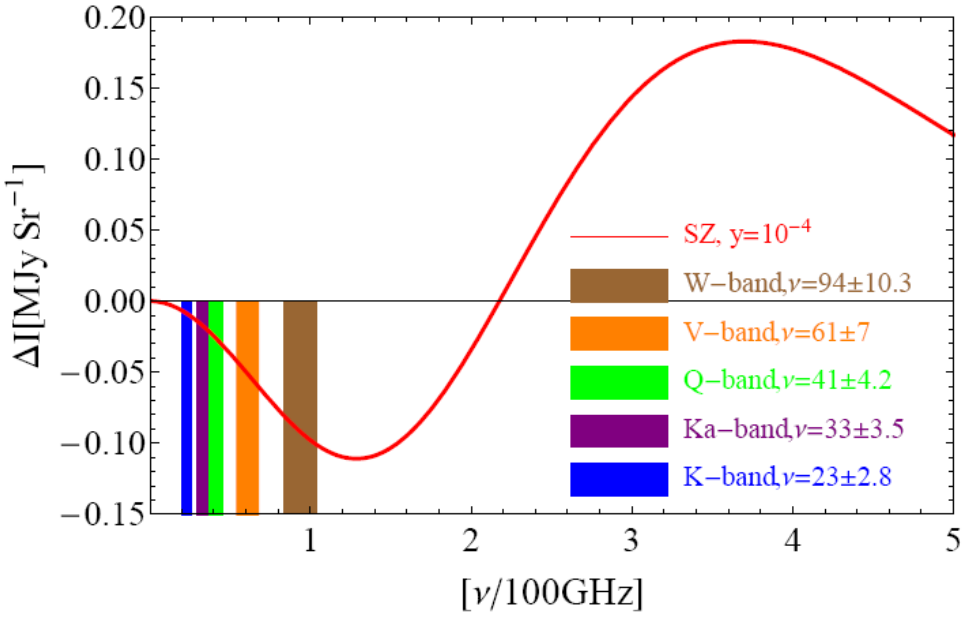
0.20
0.15
0.10
0.05
0.00
−0.05
−0.10
−0.15
ΔI[MJy Sr^{-1}]
1
2
3
4
5
[ν/100GHz]
SZ, y=10^{-4}
W−band,ν=94±10.3
V−band,ν=61±7
Q−band,ν=41±4.2
Ka−band,ν=33±3.5
K−band,ν=23±2.8

Planck:

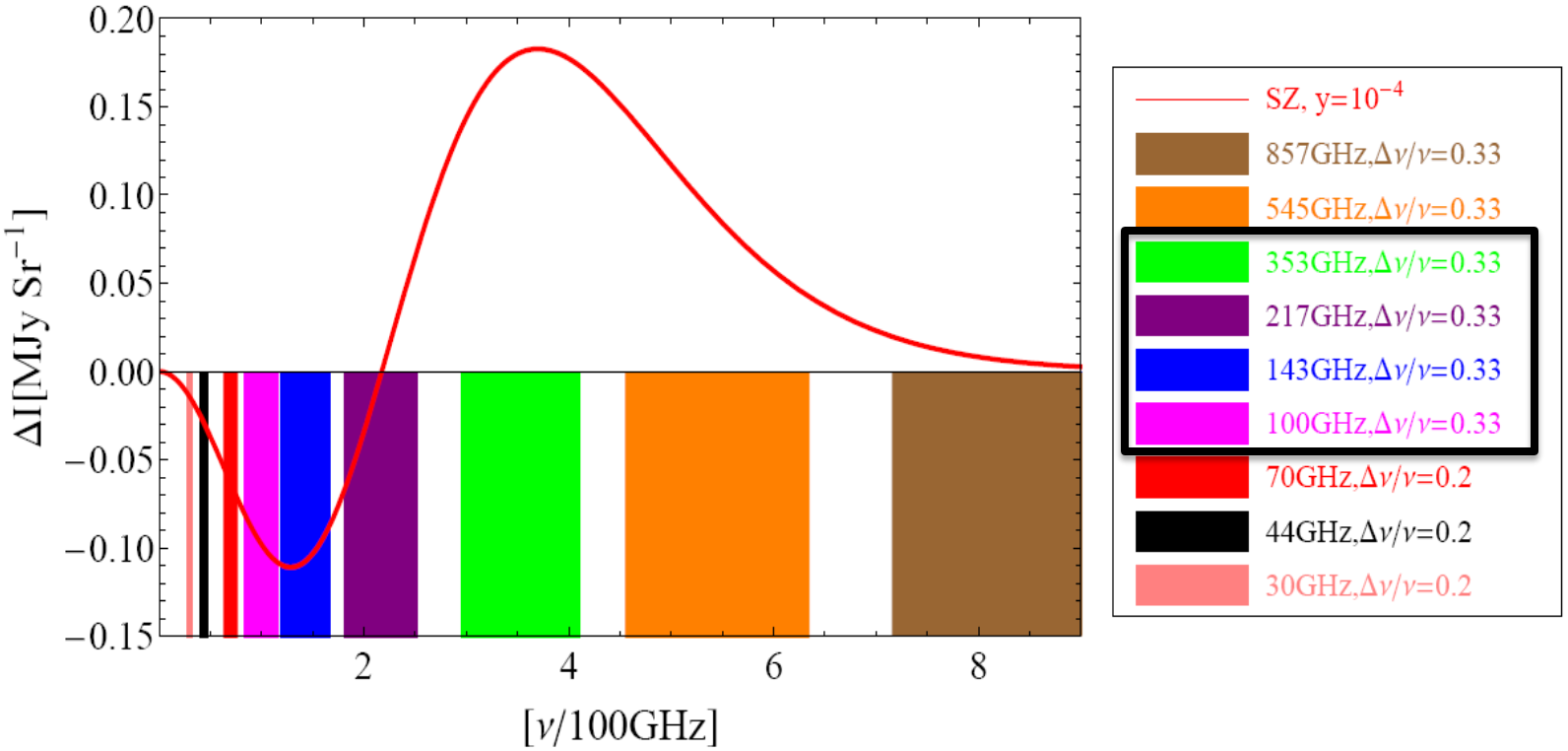
0.20
0.15
0.10
0.05
0.00
−0.05
−0.10
−0.15
ΔI[MJy Sr^{-1}]
2
4
6
8
[ν/100GHz]
SZ, y=10^{-4}
857GHz,Δν/ν=0.33
545GHz,Δν/ν=0.33
353GHz,Δν/ν=0.33
217GHz,Δν/ν=0.33
143GHz,Δν/ν=0.33
100GHz,Δν/ν=0.33
70GHz,Δν/ν=0.2
44GHz,Δν/ν=0.2
30GHz,Δν/ν=0.2

SZ map from linear combination of Planck frequency bands: ν_i = 100, 143, 217, 353 GHz.

$$T_{SZ}/T_0 \equiv y\, S_{SZ}(\nu_i) = \sum b_i\, T(\nu_i)$$

1. $\sum b_i\, S_{SZ}(\nu_i) = 1$ →0 ! $\quad S_{SZ}(x) = x\, coth(x/2) - 4 \quad (x = h\nu/kT)$

2. $\sum b_i\, S_{CMB}(\nu_i) = 0$ →1 ! $\quad S_{CMB}(x) = 1$

3. $\sum b_i\, S_{"dust"}(\nu_i) = 0 \qquad S_{"dust"}(\nu_i) = \nu^{\beta}\, g(x)$

Planck SMICA, SEVEM, NILC maps

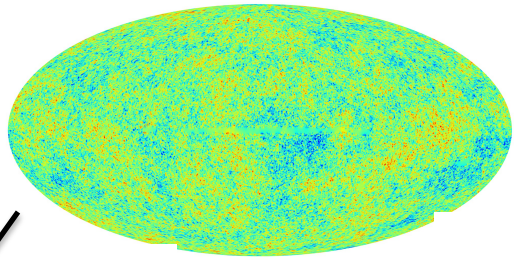

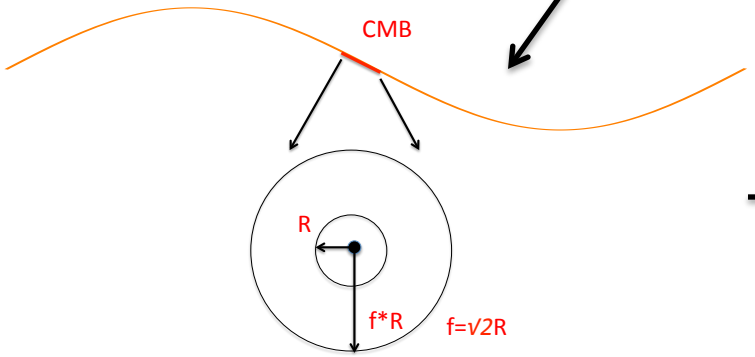

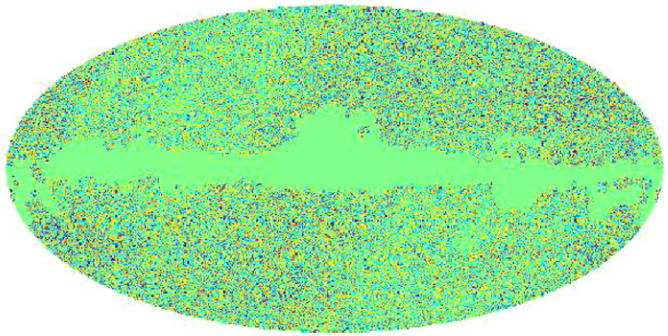

X

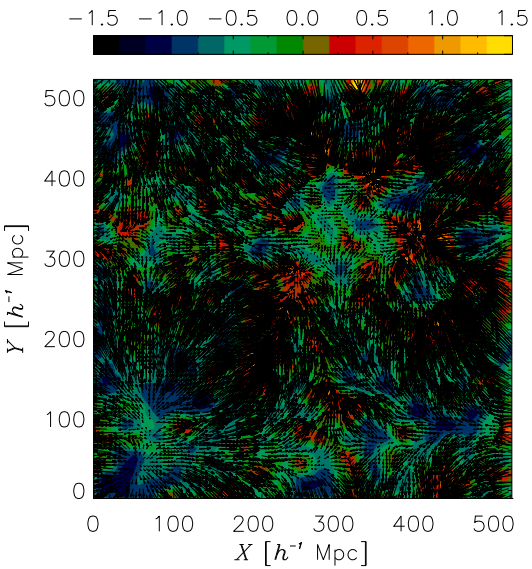

$$w^{T,v}(r) = \langle \delta T_i v_{\rm los}^{\rm rec}(\boldsymbol{x}_j) \rangle_{i,j}(r)$$

Planck SMICA, SEVEM, NILC maps

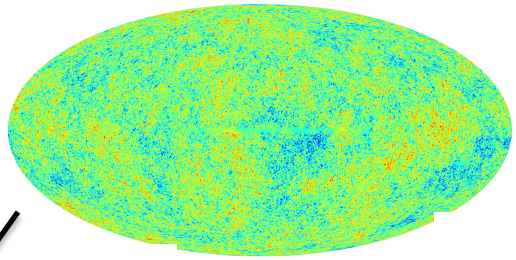

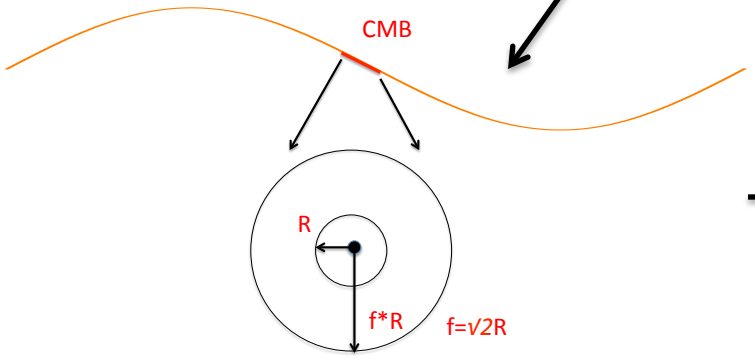

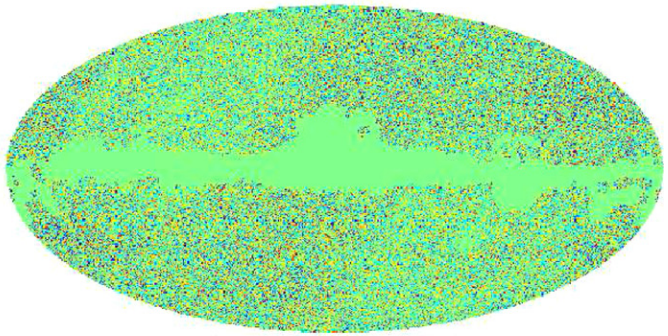

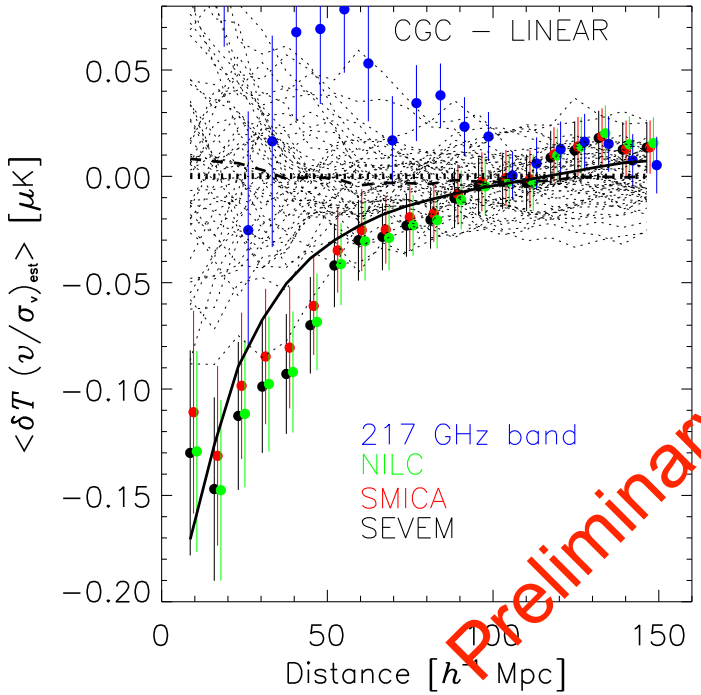

X

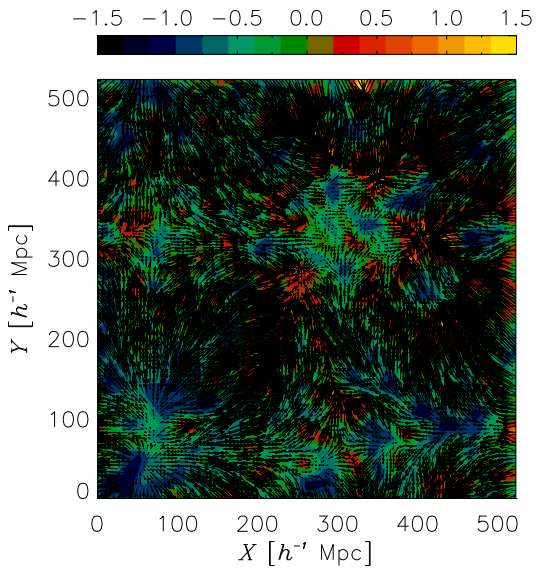

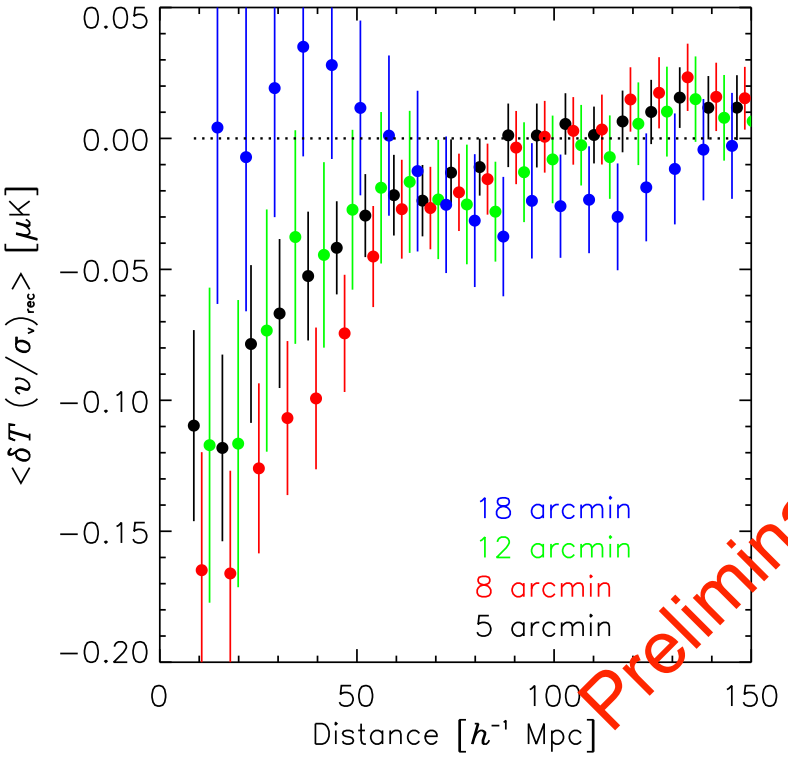
0.05
0.00
−0.05
−0.10
−0.15
−0.20
0
50
100
150
Distance [h^{-1} Mpc]
$<\delta T\ (v/\sigma_v)_{rec}>$ [μK]
18 arcmin
12 arcmin
8 arcmin
5 arcmin
Preliminary

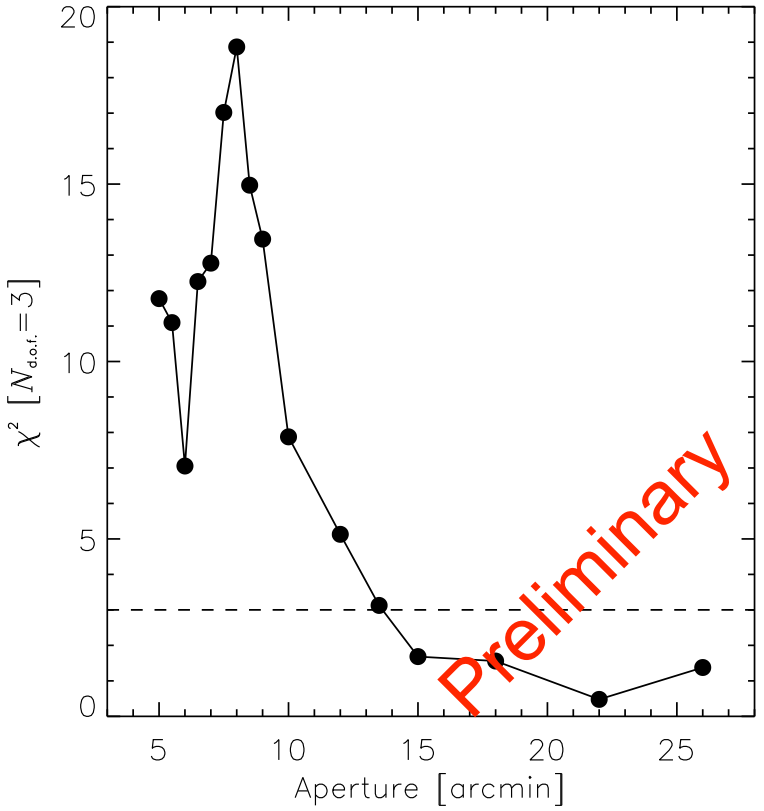
20
15
10
5
0
5
10
15
20
25
Aperture [arcmin]
χ^2 [$N_{d.o.f.}=3$]
Preliminary

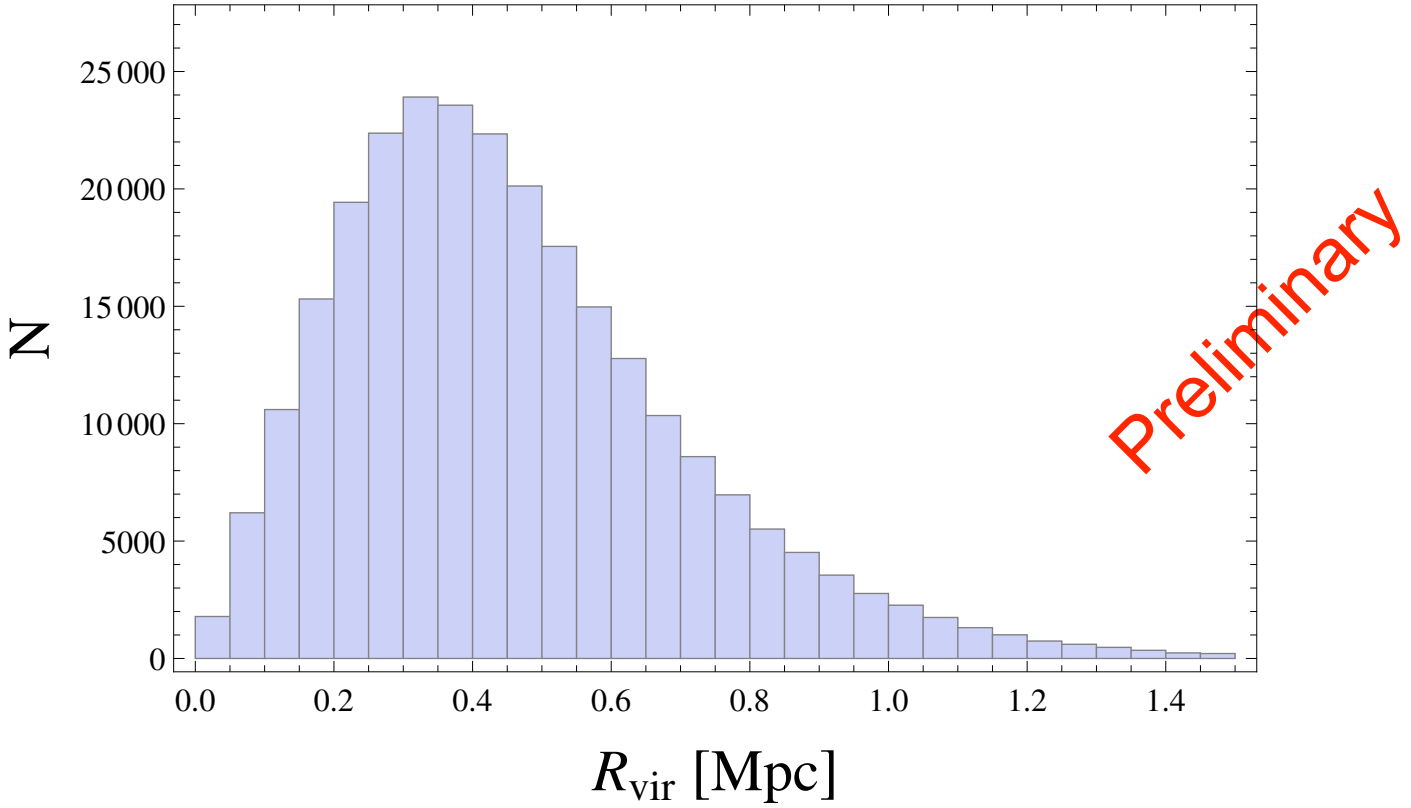

(1) An aperture of 8 arcmin for CGC sources (placed at a median redshift of *z* = 0.12) corresponds to a physical radius of roughly 1 Mpc, which is at least twice the typical virial radius of the CGs. Combining this with the behaviour of the signal for the 5, 8, and 12 arcmin apertures suggests that most of the detected kSZ signal is coming from outside the halos themselves.

(2) The full implication of the results is being investigated in terms of the average optical depth model and the halo model. The results will come out as an external paper.

Gas within/around filament

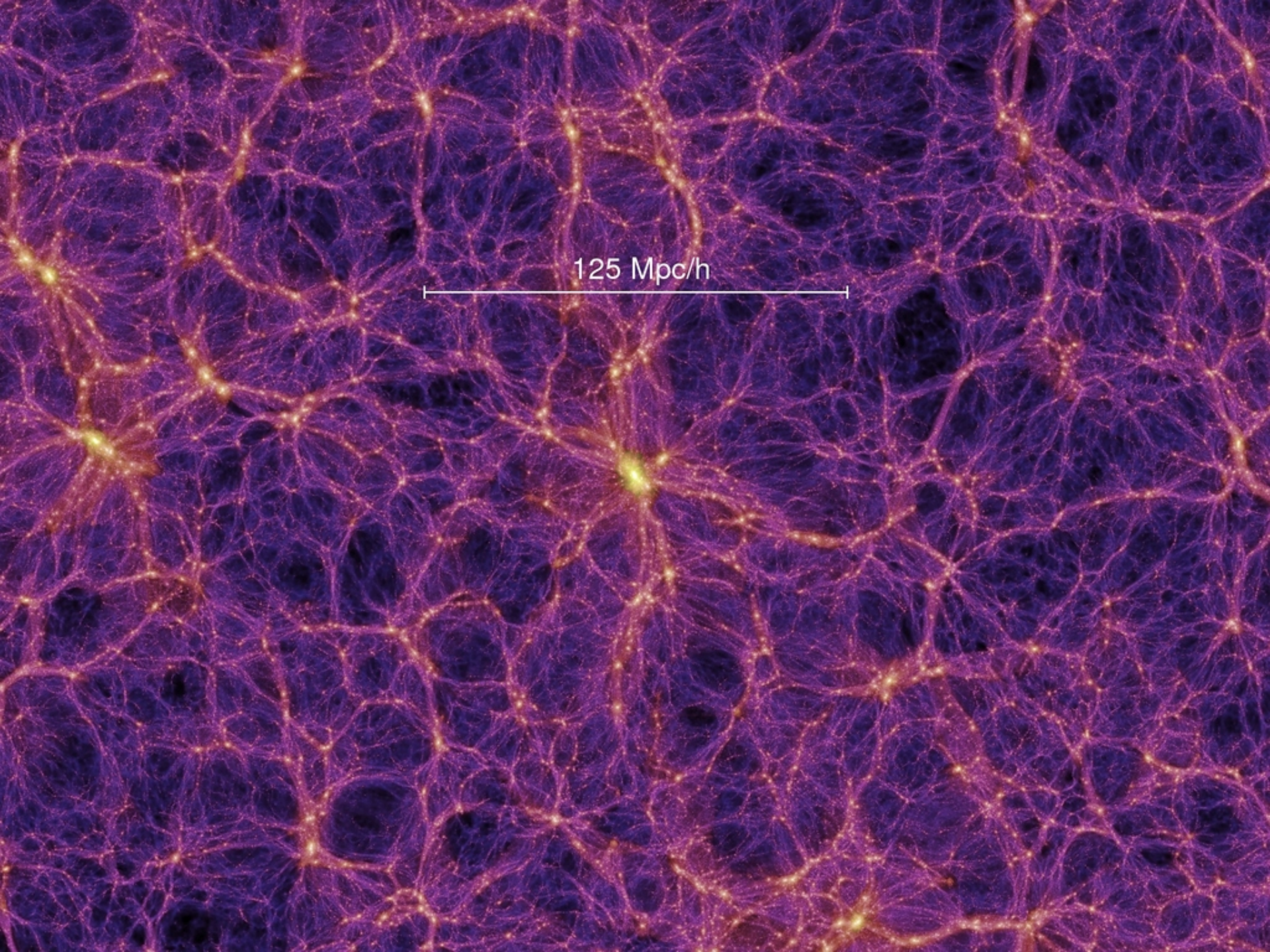
125 Mpc/h

12h
16h
8h
20h
4h
0h
0.02
0.04
0.06
0.08
0.10
0.12
0.14
Redshift z

Stacking LRG/SDSS pairs (Ms>11.3, 0.15<z<0.43 (N=28247)) on Planck y-map

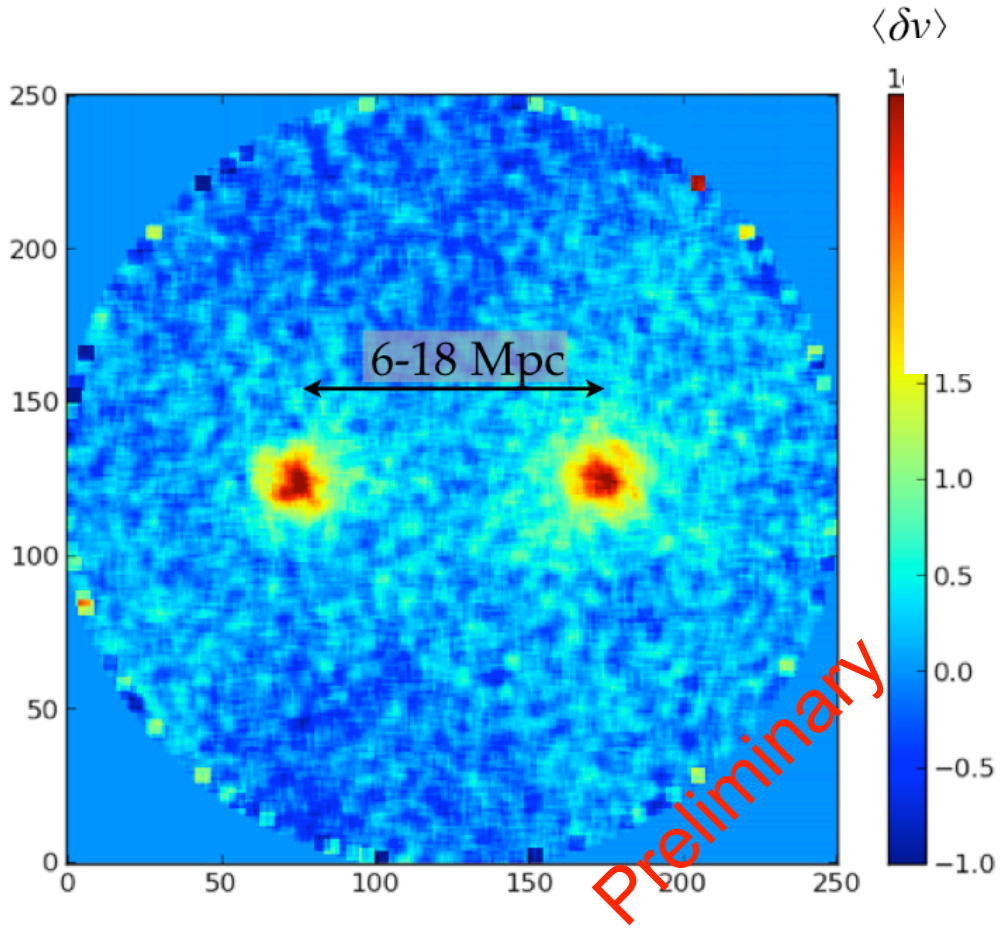

Radial distance:
+- 6 Mpc

$6\ \mathrm{Mpc} < r_{\perp} < 18\ \mathrm{Mpc}$

Question: is there evidence for a gas filament bridging the pairs?

Stacked

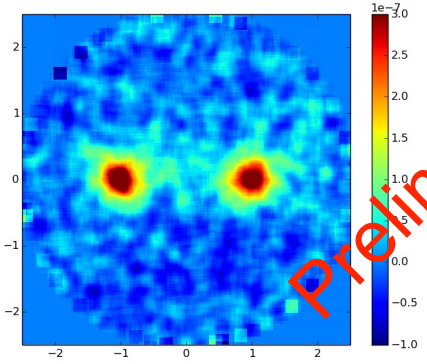

Preliminary

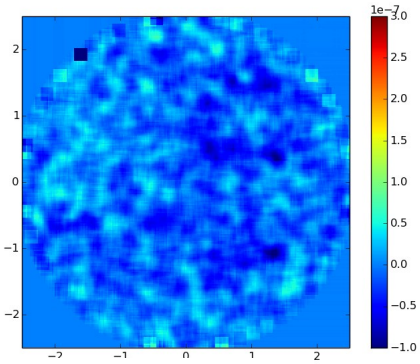

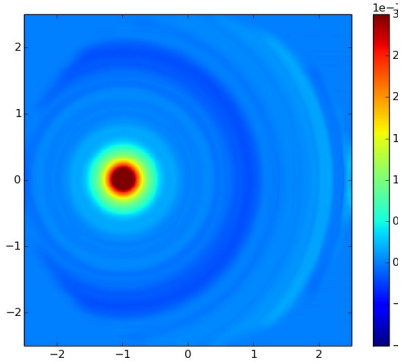

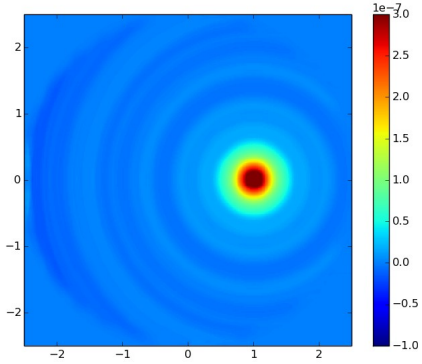

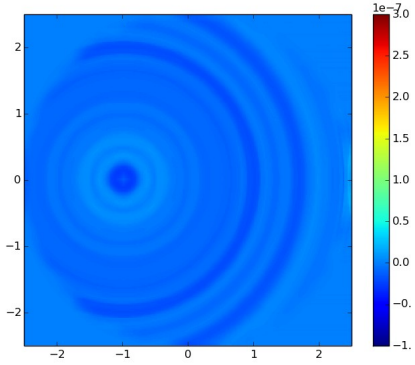

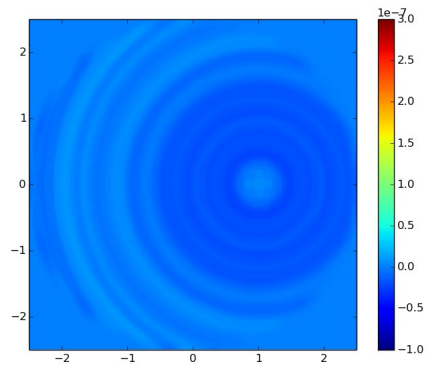

LRG SZ Subtracted

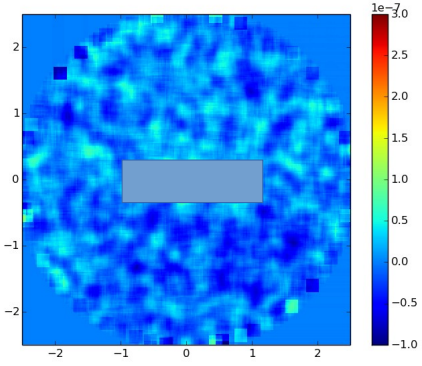

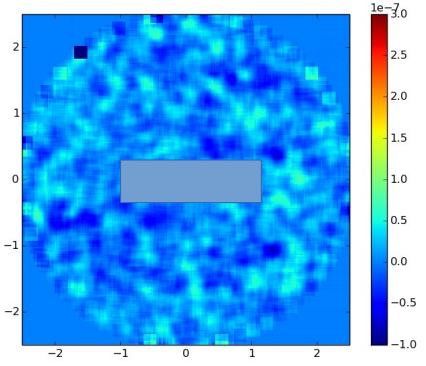

LRG SZ Subtracted

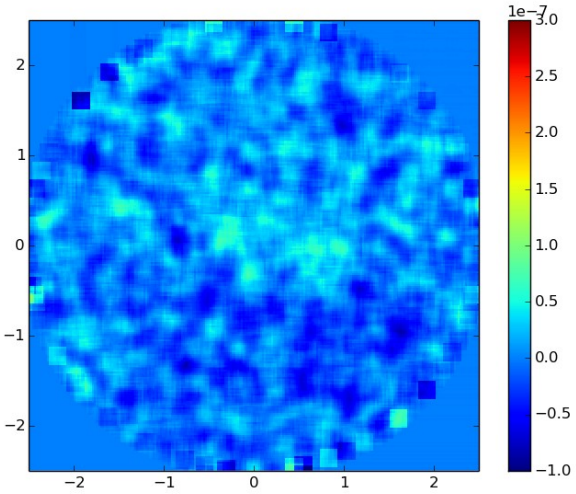

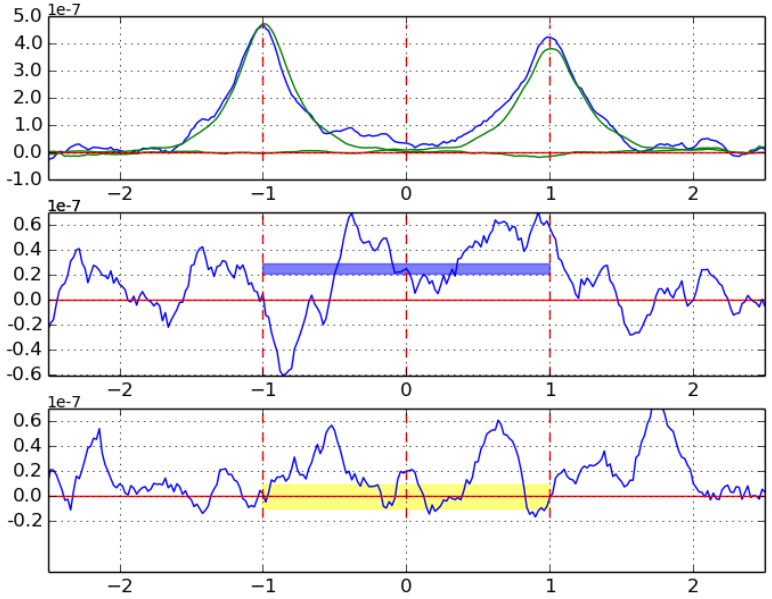

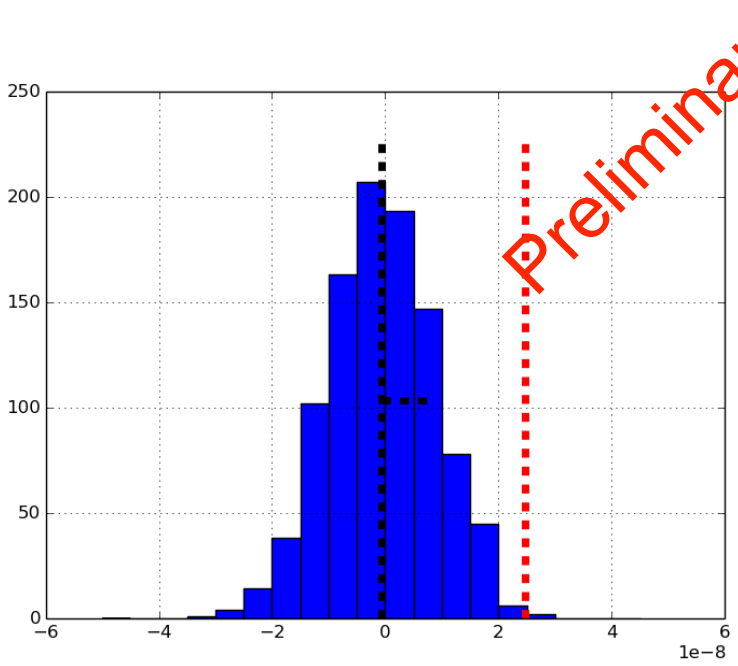

$$y = \int n_{\rm e} \sigma_{\rm T} \frac{k_{\rm B} T_{\rm e}}{m_{\rm e} c^2} {\rm d}l$$

$$n_{\rm e} = \overline{n}_{\rm e,i} (1 + \delta)$$

$$\overline{n}_{\rm e,i} = \frac{\chi \rho_{\rm b}(z)}{\mu_{\rm e} m_{\rm p}} \qquad \chi = \frac{1 - Y_{\rm p}(1 - N_{\rm H_e}/2)}{1 - Y_{\rm p}/2}$$

$$\left(\frac{T_{\rm e}}{10^7 {\rm K}}\right) \left(\frac{1+\delta}{10}\right) \left(\frac{\Delta l}{\rm Mpc}\right) = 1.41 \pm 0.53$$

Preliminary

Conclusion:

- Most of the baryons in the Universe is in a warm-hot diffuse status, for which X-ray observation is hard to measure.
- We probe gas by cross-correlating the Sunyaev-Zeldovich map from Planck with CFHTLens lensing mass maps and SDSS LRG pair catalogue to probe gas distributions that are difficult to trace.
- Significant correlation is seen with lensing mass. Data is reasonably well fit by a halo model, but requires gas out to 5 × virial radius. By the virial theorem, the temperature of this gas exactly corresponds to the 10^5—10^7K, i.e. warm-hot intergalactic medium. This is consistent with the finding from numerical simulation.
- We use the aperture photometry filter to the kSZ map, and find the maximum correlation between kSZ-velocity field is at theta=8 arcmin, corresponding to gas outside virial radius.
- We stack Planck y on the same sample and find the evidence for a “gas bridge” at the level of y = (2.46 +-0.93) × 10^{-8} (68% CL). This corresponds to the temperature of gas bridge to be less than 10^7 K.
- Our results show that the baryons are no-longer “missing” and they are neither too hot nor too cold, but correlated with underlying mass distribution (lensing and velocity field).

tial variations. Distinguishing Galactic from extragalactic dust is very difficult, as their SEDs are quite similar, and both their spatial and spectral variations do not exhibit any particular features. Currently, the best approach is to rely on a Galactic tem-

Planck 2013 Results. XXX. Cosmic infrared background measurements and implications for star formation

2014, Astronomy and Astrophysics, 571, 30